

Supporting Information for
Exploring Aporphine as Anti-inflammatory and
Analgesic Lead from *Dactylicapnos scandens*

Bei Wang^{‡,§,¶}, Yin-Jiao Zhao^{†,¶}, Yun-Li Zhao^{†,‡,¶}, Ya-Ping Liu[‡], Xiao-Nian Li[‡], Hong-Bin Zhang^{†,*}, and Xiao-Dong Luo^{†,‡,*}

[†]Key Laboratory of Medicinal Chemistry for Natural Resource, Ministry of Education and Yunnan Province, School of Chemical Science and Technology, Yunnan University, Kunming 650091, China

[‡]State Key Laboratory of Phytochemistry and Plant Resources in West China, Kunming Institute of Botany, Chinese Academy of Sciences, Kunming, 650201, China

[§]Key Laboratory of Screening and Processing in New Tibetan Medicine of Gansu Province, School of Life Science and Engineering, Lanzhou University of Technology, Lanzhou 730050, China.

Contents

1. Plant material	1
2. Extraction and isolation	1
3. Table S1. ¹ H and ¹³ C NMR Spectral Data (δ in ppm) of 1 and 2	3
4. Total synthesis of dactylicapnosine A	4
4.1 Sheme S1: Total synthesis of dactylicapnosine A	4
4.2 Experimental details and characterization data	4
5. Evaluation of anti-inflammatory activity <i>in vitro</i>	14
5.1. Effects on cell viability of RAW 264.7	14
Table S2. Effect of dactylicapnosines on cell viability after 24 h treatment.	14
5.2 Effect on the production of inflammatory cytokines <i>in vitro</i>	15
Table S3. Effects of dactylicapnosines on the production of cytokines in LPS-induced RAW 264.7 cells	15
6. Evaluation of anti-inflammatory and analgesic <i>in vivo</i>	16
6.1 Effect on xylene-induced inflammation in mice.	16
Table S4. Effects of dactylicapnosine A on auricle swelling induced by xylene in mice.	17
6.2 Effect on acetic acid-induced pain in mice.	17
Table S5. The analgesic effect of dactylicapnosine A in mice induced by acetic acid	18
6.3 Effect on formaldehyde-induced pain in mice.	18
Table S6. The analgesic effect of dactylicapnosine A in mice induced by formaldehyde	19
6.4 Effect on hotplate-induced pain in mice.	19
Table S7. The analgesic effect of dactylicapnosine A in mice induced by hotplate	20
6.5 Ethical approvals of experimental animals.	21
Reference	22
7. Supplementary Figures	23
Figure S01. The HPLC profiles of separation of (+)- 1 and (-)- 1	23
Figure S02. The HPLC profiles of separation of (+)- 2 and (-)- 2	24
Figure S03. The overlapped experimental CDs of compounds (+)- 2 and (-)- 2	24
Figure S04. ¹ H NMR spectrum of compound 1 (CDCl ₃ /CD ₃ OD)	25
Figure S05. ¹³ C NMR and DEPT spectra of compound 1 (CDCl ₃ /CD ₃ OD)	26
Figure S06. HSQC spectrum of compound 1 (CD ₃ OD)	27
Figure S07. HMBC spectrum of compound 1 (CD ₃ OD)	28
Figure S08. HREIMS spectrum of compound 1	29
Figure S09. ESIMS spectrum of compound 1	30
Figure S10. IR spectrum of compound 1	31
Figure S11. UV spectrum of compound 1	32
Figure S12. CD spectrum of compound (+)- 1	33
Figure S13. CD spectrum of compound (-)- 1	35
Figure S14. ¹ H NMR spectrum of compound 2 (CDCl ₃)	37
Figure S15. ¹³ C NMR and DEPT spectra of compound 2 (CDCl ₃)	38

Figure S16. HSQC spectrum of compound 2 (CDCl ₃)	39
Figure S17. HMBC spectrum of compound 2 (CDCl ₃)	40
Figure S18. HREIMS spectrum of compound 2	41
Figure S19. ESIMS spectrum of compound 2	42
Figure S20. IR spectrum of compound 2	43
Figure S21. UV spectrum of compound 2	44
Figure S22. CD spectrum of compound (+)- 2	45
Figure S23. CD spectrum of compound (-)- 2	47
Figure S24. Copies of NMR spectra of compounds in Total synthesis.....	49
8. Crystal data and structure refinement for dactylicapnosine A (1).	63
9. ECD Calculation of dactylicapnosine A (1)	63
Table S8 Conformational population of <i>R</i> -1 at MMFF94 force field.	64
Table S9 Standard orientation of <i>R</i> -1 at B3LYP/6-311G* level in gas phase.	64
Table S10 Standard orientation of <i>R</i> -1 at B3LYP/6-311G* level in solvent phase.	66
References.....	67

1. Plant material

Air-dried roots of *D. scandens* were purchased from a market of Chinese medical materials located at Zhonghao-Luoshi-Wan of Kunming, Yunnan province, P.R. China, in February 2015. The material was identified by Dr. Ya-Ping Liu. A voucher specimen (No. 201500208) has been deposited at Kunming Institute of Botany, Chinese Academy of Sciences, Kunming, China.

2. Extraction and isolation

Air-dried roots of *D. scandens* (3.9 kg) were extracted with 80.0% MeOH/H₂O under reflux conditions, and the solvent was evaporated in vacuo. The residue was dissolved in 0.37% HCl (pH 2-3) and the solution was subsequently basified using 10% ammonia to pH 9-10. The basic solution was partitioned with EtOAc, affording a two-phase mixture. The EtOAc fraction (104 g) was divided into Fr. A-F by using silica gel chromatography (CHCl₃/MeOH, 1:0-2:8, v/v). Of which, Fr.C (3.5 g) was separated by RP-18 chromatography (MeOH/H₂O, 35:65-100:0) to give six portions, then Fr.C5 (0.65g) was subjected to silica gel chromatography under isocratic conditions (Petroleum ether/Acetone, 10:1, v/v), Sephadex LH-20 (CHCl₃/MeOH) and recrystallized to yield **1** (8.9 mg) and subfractions. Among them, Fr.C5-2 (0.1 g) was eluted through silica gel chromatography (Petroleum ether/ Acetone, 5:1, v/v) to afford **2** (8.4 mg).

Compounds **1** and **2** were further purified by HPLC equipped with a chiralphase column (Reposil chiral-AM, 5 μ m, 250mm*4.6mm r65am. S2546 (Dr. maisch)), (n-hexane/ethanol, 80:20, 1.0 mL/min; n-hexane/ethanol, 70:30, 1.0 mL/min) to give (-)-**1** (2.3 mg, t_R 25.5min) and (+)-**1** (2.2 mg, t_R 34.8 min), (-)-**2** (2.0 mg, t_R 33.9 min) and (+)-**2** (2.2 mg, t_R 41.8 min), respectively.

Dactylicapnosine A (**1**)

light yellow crystalline lumps (CH₃OH), mp 171.1-172.3°C, $[\alpha]_D^{18} +5.90$ (c 0.13, CH₃OH); UV (MeOH) λ_{max} (log ϵ) nm 211 (4.03), 264 (3.87), 294 (3.59), 394 (3.84); IR (KBr) ν_{max} 3436, 2947, 1739, 1709, 1583, 1526, 1463, 1166cm⁻¹; ¹H, ¹³C-NMR spectroscopic data, see Table 1; ESIMS m/z 454 [M + Na]⁺; HRESIMS m/z 431.1591 [M]⁺ (calcd for C₂₂H₂₅NO₈, 431.1580).

(+)-1a [α]²⁵_D +115 (c 0.10, CHCl₃)

(-)-1b [α]²⁵_D -118 (c 0.10, CHCl₃)

Dactylicapnosine B (2)

Pale yellow powder, [α]¹⁸_D -11 (c 0.1, MeOH); UV (MeOH) λ_{max} (log ϵ) nm 206 (4.12), 275 (3.73), 333 (3.56), 425 (3.60), 529 (3.65); IR (KBr) ν_{max} 3411, 2924, 2853, 1739, 1630, 1528, 1384, 1317, 1180 cm⁻¹; ¹H, ¹³C-NMR spectroscopic data, see Table 1; ESIMS m/z 440 [M + Na]⁺; HREIMS m/z 417.1423 [M]⁺ (calcd for C₂₁H₂₃NO₈, 417.1424).

(+)-2a [α]²⁴_D +42 (c 0.04, CH₃OH)

(-)-2b [α]²⁴_D -47 (c 0.06, CH₃OH).

3. Table S1. ^1H and ^{13}C NMR Spectral Data (δ in ppm) of **1 and **2**.**

no.	1^a	1^b		2^c		
	δ_{H} (<i>J</i> in Hz)	δ_{C}	δ_{H} (<i>J</i> in Hz)	δ_{C}	δ_{H} (<i>J</i> in Hz)	δ_{C}
1		144.1		143.7		143.0
1-OH					12.6, s	
1a		127.4		126.5		121.5
1b		118.8		117.9		116.8
2		154.0		152.0		147.5
3	7.18, s	112.7	6.93, s	111.6	6.90, s	111.6
3a		132.0		129.5		123.9
4	3.24, t, (6.4)	30.4	3.18, t, (6.5)	29.8	3.14, t, (6.5)	28.8
5	3.58, t, (6.4)	51.1	3.53, overlap	50.2	3.57, t, (6.5)	50.5
6a		154.0		152.4		154.1
7	6.48, s	96.7	6.41, s	95.8	6.38, s	96.0
7a		158.2		155.4		157.5
8		172.7		171.3		170.9
9		82.8		81.1		82.4
10		103.7		101.9		101.0
11		190.7		187.6		192.2
11a		117.4		117.4		115.9
12	3.93, s	61.7	3.97, s	61.5		
13	4.02, s	56.8	4.01, s	56.4	3.99, s	56.4
14	3.19, s	40.3	3.13, s	40.3	3.21, s	40.6
15	3.65, s	53.4	3.67, s	53.5	3.71, s	53.7
16	3.54, s	52.0	3.53, s	52.0	3.52, s	52.2
17	3.46, s	51.9	3.47, s	51.6	3.51, s	51.7

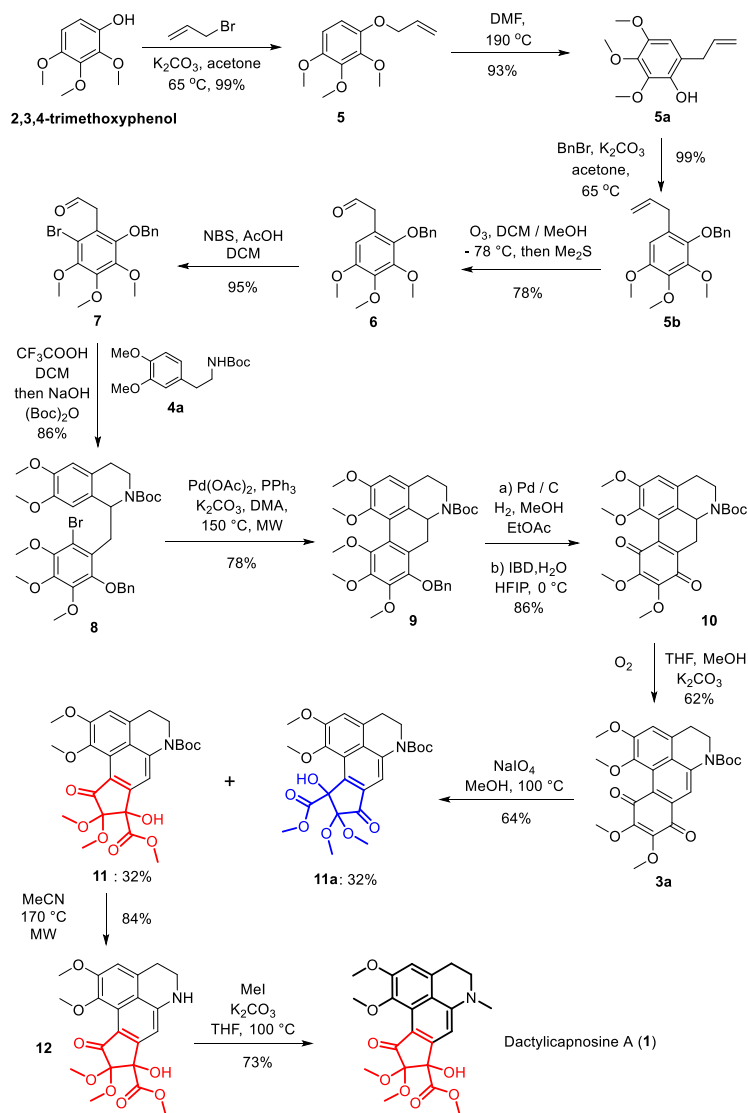
^a ^1H and ^{13}C NMR spectra were recorded at 600 and 150 MHz, respectively in CD_3OD ;

^b ^1H and ^{13}C NMR data were recorded at 500 and 125 MHz, respectively in CDCl_3 ;

^c ^1H and ^{13}C NMR data were recorded at 600 and 150 MHz, respectively in CDCl_3 .

4. Total synthesis of dactylicapnosine A

4.1 Scheme S1: Total synthesis of dactylicapnosine A

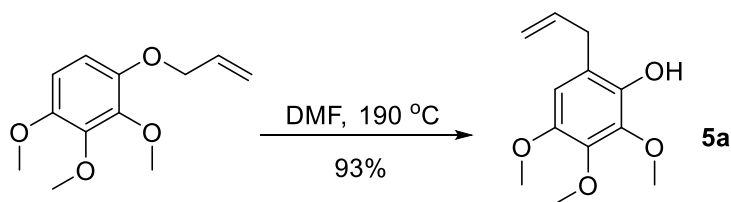


4.2 Experimental details and characterization data

Melting points were measured on a XT-4 melting-point apparatus and were uncorrected. The infrared (IR) spectra were recorded on a Nicolet iS10 FTIR spectrometer. Proton nuclear magnetic resonance (^1H -NMR) spectra were measured on Bruker Avance 300 or 400 spectrometers at 300 or 400 MHz. Carbon-13 nuclear magnetic resonance (^{13}C NMR) spectra were recorded on Bruker Avance 300 or 400 spectrometers at 75 or 100 MHz. Chemical shifts are reported as δ values in parts per million (ppm) relative to tetramethylsilane (TMS). High Resolution Mass spectra were

measured with an Agilent LC/MSD TOF mass spectrometer. For reactions conducted under MW conditions, a SEM DISCOVER SP-D microwave reactor was used. Silica gel (200–300 mesh) for column chromatography and silica GF₂₅₄ for TLC were produced by Merch Chemicals Co. Ltd. (Shanghai). Toluene and THF used in the reactions were dried by distillation over metallic sodium and benzophenone. Dichloromethane was distilled from calcium hydride or P₂O₅. Starting materials and reagents used in reactions were obtained commercially from Acros, Aldrich, Adamas-beta®, and were used without purification, unless otherwise indicated. All moisture-sensitive reactions were conducted in oven-dried glassware under a positive pressure of dry nitrogen or argon. Reagents and starting materials were accordingly transferred via syringe or cannula. Unless otherwise stated, all other reactions were performed under a positive nitrogen atmosphere. Reaction temperatures refer to the external oil bath temperature.

Compound 5a



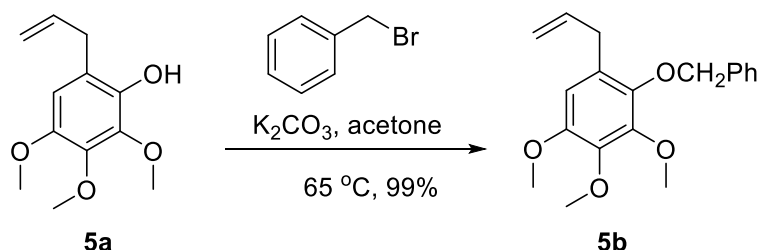
Allyl ether (3.0 g) in dry DMF (4 mL) in a sealed tube allowed to stir at 190 °C for 16 h. After this time, the reaction mixture allowed to cool to room temperature and diluted with water (80 mL). The resulting mixture was extracted with EtOAc (4 × 20 mL), and the combined organic phases were washed with brine (15 mL) and dried over anhydrous MgSO₄. After being filtered and concentrated under reduced pressure, the residue was purified by flash chromatography on silica gel (petroleum ether/ethyl acetate = 10:1) to give phenol **5a** (2.7g, 93%) as a pale yellow syrup.

The spectral data are consistent with those reported in the literature (Bochicchio, A.; Cefola, R.; Choppin, S.; Colobert, F.; Di Noia, M. A.; Funicello, M.; Hanquet, G.; Pisano, I.; Todisco, S.; Chiumminto, L. Selective Claisen rearrangement and iodination for the synthesis of polyoxygenated allyl phenol derivatives. *Tetrahedron Lett.* **2016**, 57, 4053–4055).

¹H NMR (400 MHz, CDCl₃): δ 6.44 (s, 1H), 6.04–5.94 (m, 1H), 5.49 (s, 1H), 5.12–5.05 (m, 2H), 3.95 (s, 3H), 3.87 (s, 3H), 3.80 (s, 3H), 3.36 (d, *J* = 6.4 Hz, 2H);

¹³C NMR (100 MHz, CDCl₃): δ 146.4, 140.9, 140.5, 140.3, 136.7, 120.1, 115.7, 108.6, 61.4, 61.1, 56.7, 34.1.

Compound 5b



To a solution of phenol **5a** (16.95 g, 75.6 mmol) in acetone (200 mL), K₂CO₃ (52.24 g, 378 mmol) was added followed by benzyl bromide (11 mL, 90.72 mmol). The resulting mixture was stirred at 65 °C (oil bathed) for 36 h. After being cooled to room temperature, the mixture was filtered through a short column of silica gel and washed with ethyl acetate. The filtrate was concentrated and the residue was purified by silica gel column chromatography (petroleum ether/ethyl acetate = 20:1) to give the product (**5b**, 23.51 g, 99%) as a colorless syrup.

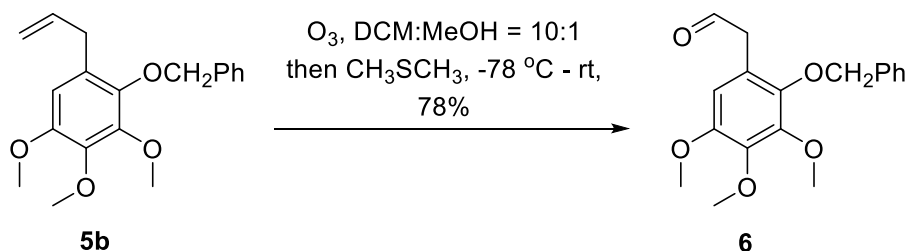
¹H NMR (400 MHz, CDCl₃): δ 7.47-7.31 (m, 5H), 6.45 (s, 1H), 5.94-5.84 (m, 1H), 5.05 (d, *J* = 13.2 Hz, 2H), 4.95 (s, 2H), 3.95 (s, 3H), 3.90 (s, 3H), 3.83 (s, 3H), 3.33 (d, *J* = 6.4 Hz, 2H);

¹³C NMR (100 MHz, CDCl₃): δ 149.6, 147.4, 144.1, 141.5, 137.9, 137.3, 128.6, 128.4, 128.3, 128.1, 116.0, 107.7, 75.5, 61.4, 56.3, 34.3;

IR (KBr, thin film, cm⁻¹): 2937, 1637, 1586, 1490, 1461, 1431, 1413, 1374, 1341, 1231, 1191, 1127, 1078, 1039, 999, 915, 836, 734, 698;

HRMS (ESI⁺) *m/z* [M + Na]⁺: calcd for C₁₉H₂₂NaO₄: 337.1410, found: 337.1410.

Compound 6



Olefin **5b** (3.0 g) was dissolved in MeOH (2 mL) and CH₂Cl₂ (20 mL). The solution was then cooled to -78 °C. A stream of ozone was passed through the solution (ca. 15 min, progress was monitored by TLC). The excess ozone was removed by a stream of oxygen (5 min), and dimethyl sulfide (4 mL) was added. The resulting mixture allowed to stir at room temperature

for 12 h. After removal of the solvent, the residue was purified by flash chromatography on silica gel (petroleum ether/ethyl acetate = 5:1) to give aldehyde **6** (2.35 g, 78%) as pale- yellow oil.

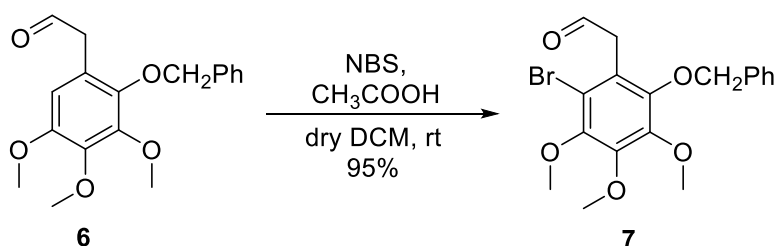
¹H NMR (400 MHz, CDCl₃): δ 9.53 (t, *J* = 2.0 Hz, 1H), 7.40-7.30 (m, 5H), 6.40 (s, 1H), 4.98(s, 2H), 3.96 (s, 3H), 3.92(s, 3H), 3.81 (s, 3H), 3.52(d, *J* = 2.0 Hz, 2H);

¹³C NMR (100 MHz, CDCl₃): δ 199.6, 149.8, 147.5, 144.5, 142.7, 137.3, 128.6, 128.5, 128.2, 120.7, 108.5, 75.4, 61.3, 56.2, 45.2;

IR (KBr, thin film, cm⁻¹): ν 2938, 2840, 2720, 1720, 1586, 1491, 1460, 1432, 1415, 1375, 1347, 1233, 1127, 1087, 1041, 997, 916, 837, 755, 699, 503;

HRMS (ESI⁺) *m/z* [M + Na]⁺: calcd for C₁₈H₂₀NaO₅: 339.1203, found: 339.1201.

Compound 7



To a solution of aldehyde **6** (8.0 g, 25.32 mmol) in dichloromethane (150 mL) was added *N*-bromosuccinimide (NBS, 4.956 g, 27.84 mmol). The resulting mixture was stirred at room temperature for 5 min before addition of acetic acid (5 mL). After being stirred for 1h, the reaction was quenched with water (50 mL) and the organic layer was separated. The aqueous phase was then extracted with CH₂Cl₂ (3 × 25 mL). The combined organic phases were dried over anhydrous MgSO₄. After removal of the solvents under reduced pressure, the residue purified by flash chromatography on silica gel (petroleum ether/ethyl acetate = 10:1) to afford the bromide (**7**, 9.52g, 95%) as pale yellow oil.

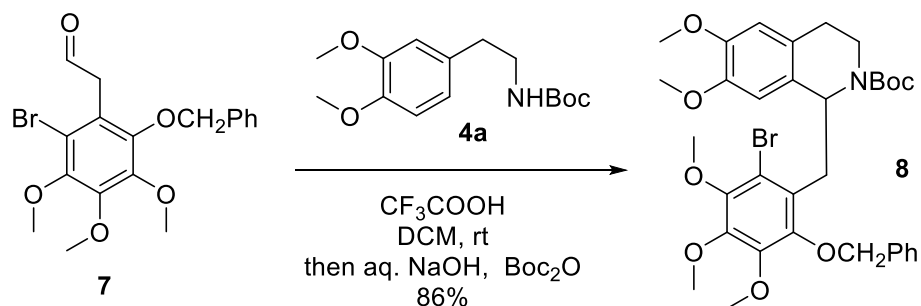
¹H NMR (300 MHz, CDCl₃): δ 9.56 (t, *J* = 1.2 Hz, 1H), 7.40-7.33 (m, 5H), 4.98 (s, 2H), 3.97 (s, 3H), 3.94 (s, 3H), 3.88 (s, 3H), 3.83(d, *J* = 1.5 Hz, 2H);

¹³C NMR (75 MHz, CDCl₃): δ 198.6, 147.8, 147.7, 147.4, 146.7, 136.8, 128.6, 128.4, 123.0, 114.6, 75.7, 61.4, 61.3, 61.0, 45.1;

IR (KBr, thin film, cm⁻¹): 2938, 2837, 2718, 1724, 1497, 1466, 1412, 1373, 1347, 1304, 1244, 1196, 1118, 1084, 1040, 989, 919, 794, 748, 699;

HRMS (ESI⁺) *m/z* [M + Na]⁺: calcd for C₁₈H₁₉BrNaO₅: 417.0308, found: 417.0303.

Compound 8



To a solution of aldehyde **7** (9.52 g, 24.16 mmol) in dichloromethane (200 mL) was added *tert*-butyl (3,4-dimethoxyphenethyl) carbamate (**4a**, 6.18 g, 21.96 mmol). After being stirred at room temperature for 5 min, CF₃COOH (8.2 mL, 109.8 mmol) was introduced. The reaction mixture was then stirred for 3 h. After TLC, the reaction mixture was quenched by carefully addition of 5% aqueous solution of NaOH, until pH = 13-14. Boc anhydride [(Boc)₂O, 2.39 g, 10.98 mmol] was then added, and the resulting mixture was stirred at ambient temperature for 12 h. The resulting mixture was diluted with water (150 mL) and extracted with CH₂Cl₂ (3 × 100 mL). The combined organic layer was dried over anhydrous MgSO₄. After removal of the solvents, the residue was purified by flash chromatography on silica gel (petroleum ether/ethyl acetate = 5:1) to give isoquinoline **8** (12.46 g, 86%) as a syrup.

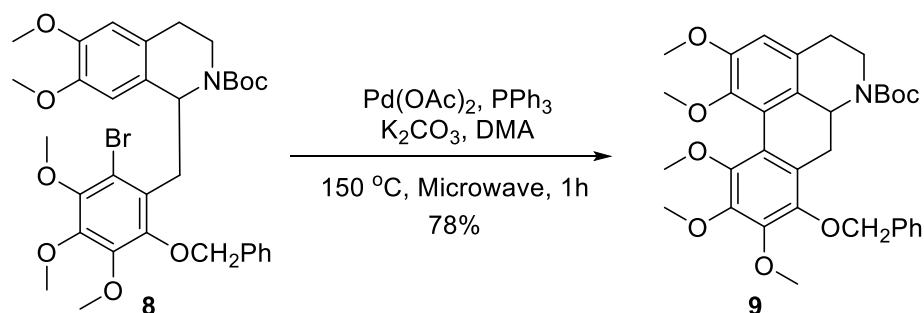
¹H NMR (400 MHz, CDCl₃): δ 7.39-7.18 (m, 5H), 6.71-6.25 (m, 2H), 5.50-5.32 (m, 1H), 5.02-4.57 (m, 2H), 4.10-4.06 (m, 1H), 3.87-3.61 (m, 14H), 3.40-2.92 (m, 4H), 2.73-2.37 (m, 2H), 1.34-1.11 (m, 9H);

¹³C NMR (100 MHz, CDCl₃): δ 154.4, 154.2, 148.4, 148.3, 147.8, 147.5, 147.3, 147.1, 146.9, 146.6, 146.5, 146.4, 146.2, 137.9, 137.6, 129.4, 129.3, 128.5, 128.0, 127.9, 127.8, 127.5, 126.9, 126.6, 120.7, 115.2, 115.1, 112.0, 111.5, 111.4, 111.2, 110.2, 109.9, 79.1, 79.0, 74.8, 74.7, 61.5, 61.4, 61.3, 61.0, 55.9, 55.8, 55.7, 53.6, 52.8, 39.0, 36.9, 36.7, 28.5, 28.4, 28.3, 28.2;

IR (KBr, thin film, cm⁻¹): 3727, 3629, 2935, 1685, 1654, 1518, 1466, 1412, 1364, 1332, 1244, 1227, 1165, 1120, 1098, 1082, 1038, 1001, 937, 859, 766, 699;

HRMS (ESI⁺) *m/z* [M + Na]⁺: calcd for C₃₃H₄₀BrNNaO₈: 680.1830, found: 680.1834.

Compound 9



Compound **8** (1.31 g, 2 mmol), palladium acetate (45 mg, 0.2 mmol), PPh_3 (534 mg, 2 mmol) and K_2CO_3 (552 mg, 4 mmol) were put into a tube. *N,N*-dimethylacetamide (20 mL) was added (operations were conducted in a nitrogen-filled glovebox). After being stirred at room temperature for 1h, the sealed vessel was removed from the glovebox, and irradiated in a microwave reactor (SEM DISCOVER SP-D, 150 W) at $150\text{ }^\circ\text{C}$ for 1h. The reaction mixture allowed to cool to room temperature, diluted with water (80 mL) and extracted with ethyl acetate ($4 \times 50\text{ mL}$). The combined organic phases were washed with brine (30 mL), dried over anhydrous MgSO_4 . After being filtered and concentrated under reduced pressure, the residue was purified by flash chromatography on silica gel (petroleum ether/ethyl acetate = 5:1) to give aporphine **9** (0.9 g, 78%) as pale yellow solid.

Melting Point: $161\text{--}162\text{ }^\circ\text{C}$;

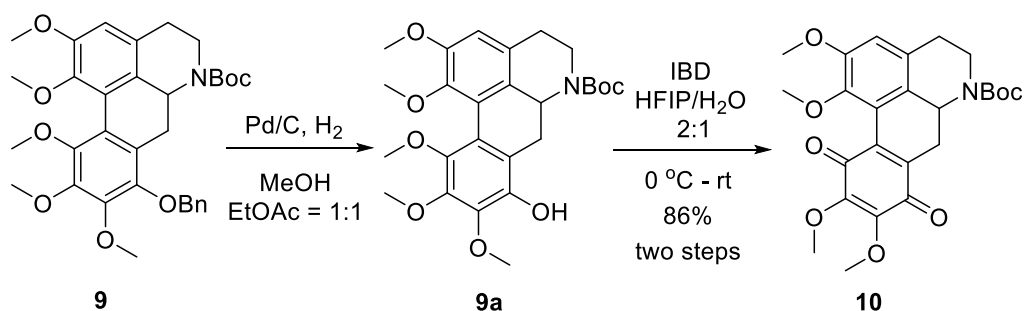
$^1\text{H NMR}$ (400 MHz, CDCl_3): δ 7.52–7.29 (m, 5H), 6.67 (s, 1H), 5.05 (d, $J = 10.0\text{ Hz}$, 1H), 4.93 (d, $J = 10.8\text{ Hz}$, 1H), 4.49 (br s, 1H), 4.39 (br s, 1H), 3.99 (s, 3H), 3.97 (s, 3H), 3.87 (s, 3H), 3.72 (s, 3H), 3.64 (s, 3H), 3.32 (dd, $J = 3.2, 13.6\text{ Hz}$, 1H), 2.92–2.81 (m, 2H), 2.67–2.61 (m, 1H), 2.19 (t, $J = 13.6\text{ Hz}$, 1H), 1.46 (s, 9H);

$^{13}\text{C NMR}$ (100 MHz, CDCl_3): δ 154.8, 151.8, 149.3, 146.8, 145.9, 145.6, 144.7, 137.8, 128.5, 128.4, 128.2, 128.0, 127.4, 127.3, 125.4, 120.2, 111.8, 80.1, 75.6, 61.5, 61.4, 61.2, 60.8, 56.1, 51.9, 38.9, 30.1, 29.5, 28.5;

IR (KBr, thin film, cm^{-1}): 3438, 2945, 1677, 1598, 1463, 1400, 1368, 1324, 1286, 1263, 1168, 1121, 1041, 1017, 1001, 975, 847, 824, 772, 755, 700;

HRMS (ESI^+) m/z $[\text{M} + \text{Na}]^+$: calcd for $\text{C}_{33}\text{H}_{39}\text{NNaO}_8$: 600.2568, found: 600.2565.

Compound 10



A mixture of the benzyl protected compound **9** (4.89 g, 8.47 mmol) and Pd/C (10%, 0.89g) in MeOH and EtOAc (40 mL, 1:1) was hydrogenated in an autoclave (0.4MPa H₂) for 24 h at room temperature. The catalyst was removed by filtered through a short column of silica gel, and the filtrate was concentrated under reduced pressure to give the crude phenol. The crude phenol **9a** was dissolved in 1,1,1,3,3,3-Hexafluoro-2-propanol and H₂O (60 mL, 2:1). After being cooled to 0 °C, iodobenzene diacetate (3.0 g, 9.32mmol) was added in portions. The resulting mixture allowed to stir at room temperature for 1h. The reaction mixture was then diluted with water (50 mL) and extracted with CH₂Cl₂ (3 × 50 mL). The combined organic layer was dried over anhydrous MgSO₄. After removal of the solvents under reduced pressure, the residue was purified by flash chromatography on silica gel (petroleum ether/ethyl acetate = 3:1) to give **10** (3.432g, 86%) as orange solid.

Melting Point: 171-172 °C;

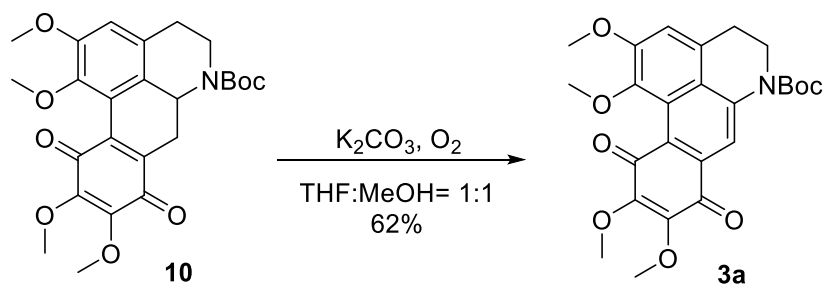
¹H NMR (400 MHz, CDCl₃): δ 6.74 (s, 1H), 4.53 (br d, *J* = 11.6 Hz, 1H), 4.40 (br s, 1H), 4.06 (s, 3H), 4.02 (s, 3H), 3.87 (s, 3H), 3.86 (s, 3H), 3.27 (dd, *J* = 4.4, 16.4 Hz, 1H), 2.85-2.74 (m, 2H), 2.65-2.59 (m, 1H), 2.19(dd, *J* = 14.4, 16.0 Hz, 1H), 1.48 (s, 9H);

¹³C NMR (100 MHz, CDCl₃): δ 182.3, 182.2, 154.6, 152.2, 146.2, 145.7, 143.5, 139.3, 138.6, 129.8, 126.5, 122.5, 114.5, 80.5, 61.3, 61.2, 60.8, 56.0, 50.7, 38.5, 29.9, 28.6, 26.0;

IR (KBr, thin film, cm⁻¹): 3443, 2926, 1678, 1648, 1600, 1481, 1406, 1366, 1286, 1204, 1163, 1130, 1107, 1018;

HRMS (ESI⁺) *m/z* [M + Na]⁺: calcd for C₂₅H₂₉NNaO₈: 494.1785, found: 494.1786.

Compound 3a



To a Schlenk flask were added *p*-quinone **10** (5.23 g, 11.11 mmol), K_2CO_3 (1.69 g, 12.22 mmol) and THF (50 mL). The resulting mixture was stirred for 10 min before addition of MeOH (50 mL). The reaction mixture was then stirred under oxygen at room temperature for about 30-40 min, and the color of the mixture changed gradually from orange to red. After TLC analysis of the reaction, the mixture was filtered, the filtrate was concentrated under reduced pressure, and the residue was purified by flash chromatography on silica gel (petroleum ether/ethyl acetate = 3:1) to afford the aporphine **3a** (3.24 g, 62%) as red solid.

Melting Point: 68-69 °C;

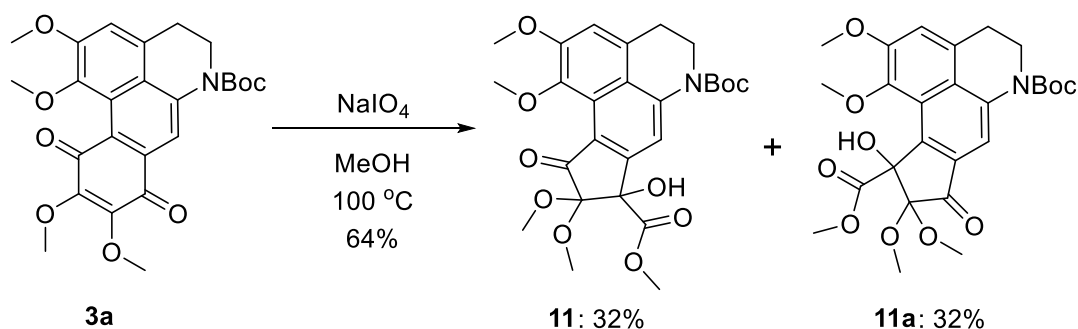
1H NMR (400 MHz, $CDCl_3$): δ 8.15 (s, 1H), 7.12 (s, 1H), 4.16 (s, 3H), 4.05-4.03 (m, 5H), 3.99 (s, 3H), 3.98 (s, 3H), 3.15 (t, $J = 5.6$ Hz, 2H), 1.56 (s, 9H);

^{13}C NMR (100 MHz, $CDCl_3$): δ 182.4, 181.9, 153.1, 151.1, 150.0, 143.4, 142.8, 141.0, 131.2, 129.2, 126.7, 125.8, 122.7, 115.7, 112.5, 82.6, 61.2, 61.0, 60.5, 56.7, 43.4, 30.3, 28.4;

IR (KBr, thin film, cm^{-1}): 3435, 2943, 1701, 1683, 1661, 1614, 1509, 1458, 1404, 1370, 1335, 1305, 1249, 1212, 1161, 1118, 1034, 982, 933, 907;

HRMS (ESI $^+$) m/z $[M + Na]^+$: calcd for $C_{25}H_{27}NNaO_8$: 492.1629, found: 492.1632.

Compound 11 and 11a



To a sealable tube (Teflon cap) were added *p*-quinone **3a** (1.341 g, 2.859 mmol), anhydrous methanol (20 mL) and $NaIO_4$ (3.045 g, 14.30 mmol). The resulting mixture was sealed and

(petroleum ether/ethyl acetate/triethylamine = 1:1:0.001→0:1:0.001) to give amine **12** (136 mg, 84%) as a yellow syrup.

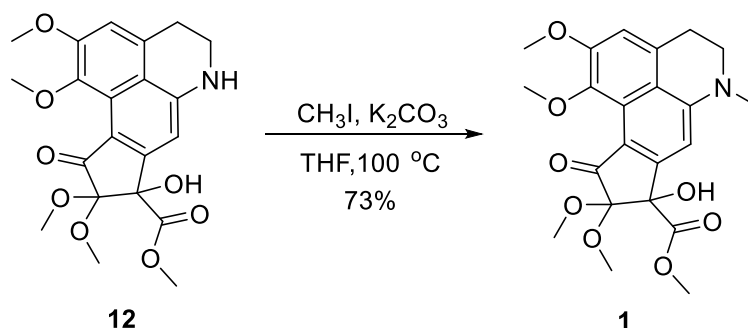
¹H NMR (300 MHz, CDCl₃): δ 6.92 (s, 1H), 6.44 (s, 1H), 5.62 (br s, 1H), 4.02 (s, 1H), 3.98 (s, 3H), 3.95 (s, 3H), 3.63 (s, 3H), 3.51-3.44 (m, 8H), 3.09 (t, *J* = 6.3 Hz, 2H);

¹³C NMR (75 MHz, CDCl₃): δ 187.5, 171.4, 155.3, 152.9, 151.8, 143.6, 130.2, 127.0, 117.4, 117.1, 112.0, 101.9, 98.3, 81.1, 61.6, 56.6, 53.5, 52.0, 51.6, 40.6, 29.6;

IR (KBr, thin film, cm⁻¹): 3330, 2942, 2836, 1697, 1592, 1525, 1458, 1416, 1394, 1342, 1306, 1256, 1161, 1041, 977, 892, 608;

HRMS (ESI⁺) *m/z* [M + Na]⁺: calcd for C₂₁H₂₃NNaO₈: 440.1316, found: 440.1316.

Dactylicapnosine A (**1**)



To a sealable tube (Teflon cap) were added amine **12** (136 mg, 0.326 mmol), K₂CO₃ (442 mg, 3.2 mmol), CH₃I (454 mg, 3.2 mmol) and THF (7 mL). The sealed reaction mixture allowed to stir at 100 °C for 36 h. After TLC analysis, the mixture was cooled to room temperature and filtered. The filtrate was concentrated under reduced pressure and the residue was purified by flash chromatography on silica gel (petroleum ether/ethyl acetate/triethylamine: 1/1/0.001, 1/2/0.001) to give amine **1** (101mg, 73%) as pale yellow plate.

Melting Point: 179-180 °C;

¹H NMR (300 MHz, CDCl₃): δ 6.91 (s, 1H), 6.39 (s, 1H), 3.99-3.94 (m, 7H), 3.65(s, 3H), 3.52-3.45 (m, 8H), 3.15 (t, *J* = 6.3 Hz, 2H), 3.10 (s, 3H);

¹³C NMR (75 MHz, CDCl₃): δ 187.6, 171.4, 155.4, 152.5, 152.0, 143.7, 129.5, 126.6, 117.9, 117.4, 111.7, 102.0, 95.8, 81.2, 61.6, 56.5, 53.5, 52.0, 51.7, 50.2, 40.4, 29.8;

IR (KBr, thin film, cm⁻¹): 3442, 2925, 1735, 1583, 1525, 1459, 1411, 1344, 1303, 1165, 1104, 1069;

HRMS (ESI⁺) *m/z* [M + Na]⁺: calcd for C₂₂H₂₅NNaO₈: 454.1472, found: 454.1472.

5. Evaluation of anti-inflammatory activity *in vitro*

ICR mice of either sex (18-22 g) were purchased from Kunming Medical University (license number SCXK 2015-0004). All animals were housed at room temperature (20-25 °C) and constant humidity (40-70%) under a 12 h light-dark cycle in SPF grade laboratory (license number SYXK 2018-0005). The experiment was reviewed and approved by the Institutional Animal Care and Use Committee of the Kunming Institute of Botany, Chinese Academy of Sciences. And the application for ethical review of experimental animals was attached. All activities related to animal care and handling were performed according to the Guide for the Care and Use of Laboratory Animals and the policies of Association for Assessment and Accreditation of Laboratory Animal Care International.

5.1. Effects on cell viability of RAW 264.7

We performed an MTT assay to evaluate the effect of dactylicapnosines treatment on the proliferation of RAW 264.7 cells. Thus, cells were treated with different concentrations (*i.e.* 100 μ M, 50 μ M and 20 μ M) for 24 hours; and results showed that cell survival was not significantly inhibited following the treatment of four compounds with the present concentrations (Table S2, $p > 0.05$) and demonstrated that dactylicapnosines had no effect on cell growth at the present concentration. Next, 100 μ M, 20 μ M and 4 μ M concentrations were selected for subsequent *in vitro* experiments.

Table S2. Effect of dactylicapnosines on cell viability after 24 h treatment.

Group	Concentration (μ M)	Survival rate (%)
Control	—	100.00 \pm 3.90
0.2% DMSO	—	91.05 \pm 0.79
isocorydine	100	89.70 \pm 7.05
	50	104.39 \pm 6.52
	20	95.48 \pm 4.13
dactylicapnosine A	100	85.23 \pm 4.53
	50	96.65 \pm 8.05
	20	97.13 \pm 2.78
(-)-dactylicapnosine A	100	92.27 \pm 1.21
	50	93.04 \pm 2.72

	20	97.86 ± 4.38
(+)-dactylicapnosine A	100	84.48 ± 4.92
	50	90.82 ± 3.33
	20	96.73 ± 3.60
(-)-dactylicapnosine B	100	81.83 ± 4.43
	50	92.38 ± 4.25
	20	87.33 ± 7.24
(+)-dactylicapnosine B	100	101.35 ± 2.92
	50	107.73 ± 3.61
	20	93.11 ± 1.86

Data were expressed as mean ± SEM. Statistical differences were represented as $p > 0.05$ vs. 0.2% DMSO

5.2 Effect on the production of inflammatory cytokines *in vitro*

PGE2, IL-1 β and TNF- α played an important role in the development of inflammation and pain. To investigate the anti-inflammatory activity of dactylicapnosines, the inflammatory cell model was constructed by LPS on RAW 264.7 cell line. As shown in Table S3, the inflammatory cytokines of PGE2, IL-1 β and TNF- α were raised after the induction of LPS compared to the control group ($p < 0.01$). Whereas the productions of TNF- α and PGE2 were decreased by isocorydine, dactylicapnosine A, and (-)-dactylicapnosine A at the concentration of 100 μ M ($p < 0.05/0.01$), interestingly, lower concentrations of (\pm)-dactylicapnosine (20 μ M and 4 μ M) also were revealed the same inhibition ($p < 0.05/0.01$). In addition, the contents of three cytokines were reduced by the treatment of (+)-dactylicapnosine A at the concentrations of 100 μ M, 20 μ M and 4 μ M ($p < 0.05/0.01$), and (-)-dactylicapnosine B only had an inhibitory effect on the secretion of TNF- α at the concentration of 100 μ M and 20 μ M ($p < 0.05$). The anti-inflammatory effects of (\pm)-dactylicapnosine A and (+)-dactylicapnosine A were similar with the positive control (DXM) at the same concentration, which encouraged us to explore the anti-inflammatory activity *in vivo*.

Table S3. Effects of dactylicapnosines on the production of cytokines in LPS-induced RAW 264.7 cells

Group	Concentration (μ M)	TNF- α (ng/L)	IL-1 β (ng/L)	PGE2 (ng/L)
Control	—	9.33 ± 0.50	2.37 ± 0.15	15.53 ± 0.32
LPS	—	14.13 ± 0.31 ^{▲▲}	3.56 ± 0.12 ^{▲▲}	22.18 ± 0.56 ^{▲▲}

DXM	20	13.04 ± 0.57	2.73 ± 0.18*	17.80 ± 0.43*
isocorydine	100	12.77 ± 0.31*	3.54 ± 0.16	19.24 ± 0.24*
	20	13.67 ± 0.55	3.46 ± 0.09	20.43 ± 0.41
	4	14.94 ± 0.27	3.50 ± 0.15	18.52 ± 0.86
dactylicapnosine A	100	13.13 ± 0.09*	3.40 ± 0.03	17.68 ± 0.12**
	20	12.95 ± 0.09*	3.29 ± 0.09	17.20 ± 0.55*
	4	13.49 ± 0.33	3.37 ± 0.07	16.73 ± 0.12**
(-)-dactylicapnosine A	100	12.95 ± 0.09*	3.23 ± 0.07	18.04 ± 0.32*
	20	14.31 ± 0.65	3.75 ± 0.40	19.24 ± 0.73
	4	13.13 ± 0.48	3.40 ± 0.07	19.00 ± 0.62
(+) -dactylicapnosine A	100	12.31 ± 0.09**	2.90 ± 0.20*	17.32 ± 0.52*
	20	12.68 ± 0.09*	2.94 ± 0.10*	17.68 ± 0.73*
	4	12.50 ± 0.16**	3.15 ± 0.10	16.97 ± 0.43**
(-)-dactylicapnosine B	100	13.04 ± 0.16*	3.46 ± 0.12	19.00 ± 0.83
	20	12.86 ± 0.09*	3.33 ± 0.04	18.88 ± 0.63
	4	13.31 ± 0.31	3.48 ± 0.12	19.12 ± 0.63
(+) -dactylicapnosine B	100	13.76 ± 1.13	3.46 ± 0.10	18.16 ± 1.06
	20	13.49 ± 0.18	3.42 ± 0.02	18.64 ± 1.26
	4	13.22 ± 0.18	3.58 ± 0.15	20.55 ± 0.84

Data were expressed as mean ± SEM. Statistical differences are represented as ▲▲ $p < 0.01$ vs Control;

* $p < 0.05$, ** $p < 0.01$ vs LPS. DXM (dexamethasone) was used as a positive control.

6. Evaluation of anti-inflammatory and analgesic *in vivo*

6.1 Effect on xylene-induced inflammation in mice.

Edema, a typical feature of inflammatory reaction, is caused by the vasodilation and the infiltration of inflammatory factors.⁸ Edematous changes such as the increased weight of ear and foot tissues can be induced by the xylene, croton oil and carrageenan. In our present work, the auricular swelling model caused by xylene was adopted to estimate the anti-inflammatory effect of dactylicapnosines *in vivo*. Results showed that intraperitoneal injection of dactylicapnosine A (10, 2 mg/kg) elicited a sharp decrease in the swelling degree by 53.30% and 54.98% compared with the control group ($p < 0.01$, Table S4), which were superior to the positive control (Parecoxib, 10 mg/kg). Meantime, the inhibition ratio of isocorydine was 44.21% (2 mg/kg) which was lower than the equivalent dose of dactylicapnosine A. The results suggested that dactylicapnosine A could remarkably inhibit the formation of edema and reduce

the weight of ear tissues, exhibiting higher inflammation-alleviating activity than isocorydine against acute inflammation. Furthermore, the most important mediators involved in the edema were prostaglandins, histamine and pro-inflammatory cytokines. It was assumed that at least some of these mediators were the subject of inhibition by dactylicapnosine A, which were in good agreement with the results previously obtained *in vitro* experiments.

Table S4. Effects of dactylicapnosine A on auricle swelling induced by xylene in mice

Group	Dose (mg/kg)	Auricular swelling (mg)	Inhibition ratio (%)
Control	—	24.5 ± 2.3	—
Parecoxib	10	20.4 ± 2.7	16.76
isocorydine	10	18.5 ± 2.2	24.71
	2	13.7 ± 2.0**	44.21
dactylicapnosine A	10	11.5 ± 1.7**	53.30
	2	11.0 ± 2.1**	54.98

Data were expressed as mean ± SEM. Statistical differences were represented as * $p < 0.05$, ** $p < 0.01$ vs. control. Parecoxib was used as a positive control.

6.2 Effect on acetic acid-induced pain in mice.

Inflammation was usually accompanied by pain and oedema as a result of increased vascular permeability and an accumulation of leukocytes and macrophages at the inflammatory site. Most anti-inflammatory drugs work as analgesics while reducing inflammation.⁹ In the present study, the acetic acid induced writhing test, formaldehyde-caused assay and hotplate experiment were performed in ICR mice to evaluate the pain-relieving effects of dactylicapnosines. The effects of dactylicapnosine A on acetic acid-induced pain were shown in Table S5. Intraperitoneal treatment with 10, 2 mg/kg of dactylicapnosine A caused a significant inhibition on the number of body-twisting frequency from 20.3 ± 4.5 (control group) to 9.3 ± 2.4 and 10.2 ± 0.9 ($p < 0.05$), respectively, which were even comparable with isocorydine (10 mg/kg, 7.8 ± 3.0; 2mg/kg, 8.6 ± 2.9) and weaker than the positive control

(morphine). The acetic acid-induced writhing response test is classical methods widely used to evaluate peripheral analgesic activities of drugs, which are affected by the release of endogenous mediators such as histamine, serotonin, bradykinin and prostaglandins. Our preliminary findings indicated that dactylicapnosine A exerted a peripheral analgesic activity, which might be attributed to endogenous mediators like TNF- α , IL-1 β and PGE2.

Table S5. The analgesic effect of dactylicapnosine A in mice induced by acetic acid

Group	Dose (mg/kg)	N	Number of writhing	Inhibition ratio (%)
Control	—	11	20.3 \pm 4.5	—
Morphine	10	11	8.5 \pm 3.0*	58.30
isocorydine	10	11	7.8 \pm 3.0*	61.43
	2	11	8.6 \pm 2.9*	57.40
dactylicapnosine A	10	11	9.3 \pm 2.4*	54.26
	2	11	10.5 \pm 3.0	48.43

Data were expressed as mean \pm SEM. Statistical differences were represented as * p < 0.05, ** p < 0.01 vs. control. Morphine was used as a positive control.

6.3 Effect on formaldehyde-induced pain in mice.

The phlogistic agent——formaldehyde, injected locally into the animal paws can induce a severe inflammation response in a biphasic response manner.¹⁰ The first phase is attributed to the release of histamine, serotonin and similar substances from damaged tissues. The second phase is mainly due to the enhanced production of kinin-like substances including prostaglandins, lysosome and proteases, and the involvement of nitric oxide, free radicals and cyclo-oxygenases in the hind paw exudate. The cumulative time of licking paws caused by formaldehyde in mice were shown in Table S6. The licking time of control group were 126.6 \pm 17.8 seconds, 188.8 \pm 24.0 seconds during the first phase (0-5 min) and the second phase (15-30 mins). However, pretreatment with isocorydine and dactylicapnosine A caused a notable reduction in hind paw licking time at both phases (p < 0.05/0.01). Isocorydine at 10 and 2 mg/kg

significantly reduced it by 38.70% and 41.79% during the first phase, and by 50.16%, 49.89% during the second phase, respectively. Similarly, the inhibition ratios of dactylicapnosine A were 39.10%, 32.94% in the first phase and 46.50%, 54.13% during the second phase at doses of 10 mg/kg and 2 mg/kg, respectively. According to our results, both isocorydine and dactylicapnosine A showed marked inhibitory activity at the first as well as second phase, which hinted the analgesic effect of it might be related with the inhibition of inflammatory cytokines.

Table S6. The analgesic effect of dactylicapnosine A in mice induced by formaldehyde

Group	Dose (mg/kg)	N	First phase (s)	Inhibition (%)	Second phase (s)	Inhibition ratio (%)
Control	—	10	126.6 ± 17.8	—	188.8 ± 24.0	—
Morphine	10	10	30.0 ± 9.7**	76.30	22.6 ± 9.2**	88.03
isocorydine	10	10	77.6 ± 14.7*	38.70	94.1 ± 22.0**	50.16
	2	10	73.7 ± 11.3*	41.79	94.6 ± 14.0**	49.89
dactylicapnosine A	10	10	77.1 ± 10.1*	39.10	101.0 ± 22.9*	46.50
	2	10	84.9 ± 15.2	32.94	86.6 ± 12.9**	54.13

Data were expressed as mean ± SEM. Statistical differences were represented as * $p < 0.05$, ** $p < 0.01$ vs. control. Morphine was used as a positive control.

6.4 Effect on hotplate-induced pain in mice.

Hot plate test, a classical method, was used to inflict heat-induced pain in mice for measurement of pain threshold. Results of the effects of dactylicapnosines on hotplate pain were depicted in Table S7. The basal threshold was approximately 20 seconds and it was recorded at 30 min, 60 min, 90 min and 120 min following the intraperitoneal administration of dactylicapnosines. There was no significant change at all-time points except that it was prolonged from 18.2 ± 1.2 to 29.7 ± 3.3 seconds at 60 min after the intervention of dactylicapnosine A at the dose of 10 mg/kg ($p < 0.01$). The positive morphine at 10 mg/kg manifested its maximum thresholds of 41.5 seconds, 33.9 seconds at 30 min and 60 min, respectively. The mechanism of the licking reaction to this nociceptive stimulus is closely related with the prostanoid system including the increased peritoneal fluid level of PGE2 and

and Prostaglandin F2a (PGF2a).¹¹ It was speculated that dactylicapnosine A might play a role in the inhibition of prostaglandin synthesis, which had been confirmed by our inflammatory cell model caused by LPS and the level of PGE2 decreased significantly.

Table S7. The analgesic effect of dactylicapnosine A in mice induced by hotplate






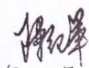
Group	Dose (mg/kg)	N	Pain thresholds (seconds)				
			0 min	30 min	60 min	90 min	120 min
Control	—	13	21.1 ± 1.6	19.8 ± 1.1	18.2 ± 1.2	24.7 ± 2.6	25.5 ± 2.8
Morphine	10	13	21.2 ± 1.3	41.5 ± 2.8**	33.9 ± 4.1**	25.3 ± 3.7	26.7 ± 1.9
isocorydine	10	13	19.9 ± 1.6	22.3 ± 1.4	22.5 ± 3.1	25.7 ± 2.6	25.9 ± 2.2
dactylicapnosine A	2	13	20.5 ± 1.3	22.0 ± 1.8	20.8 ± 1.4	20.5 ± 1.6	23.8 ± 2.0
	10	13	20.0 ± 0.8	17.2 ± 1.2	29.7 ± 3.3**	19.9 ± 1.9	32.7 ± 4.1
	2	13	19.2 ± 1.2	17.9 ± 1.4	22.8 ± 2.1	22.5 ± 2.5	25.6 ± 3.9

Data were expressed as mean ± SEM. Statistical differences were represented as * $p < 0.05$, ** $p < 0.01$ vs. control. Morphine was used as a positive control.

6.5 Ethical approvals of experimental animals.

昆明植物研究所动物实验伦理审查申请书

申请部门: 植化室		申请日期: 2018 年 12 月 10 日	
课题名称: (±)-dactylicapnosine A 和 isocorydine 小鼠二甲苯耳廓肿胀实验			
申请人姓名: 赵云丽		技术职称: 高级工程师	
岗位证书编号: KIB2017011808			
课题负责人: 罗晓东		技术职称: 研究员 联系电话: 13888333553	
申请部门负责人: 熊文勇			
拟进 动物 情况	动物来源: 昆明医科大学		
	品种: 小鼠 品系: ICR 等级规格: SPF 级		
	数量: 64 只(♀ 32 只; ♂ 32 只)		申购日期: 2018 年 12 月 10 日
	进驻日期: 2018 年 12 月 13 日		结束日期: 2018 年 12 月 20 日
<p>实验要点,包括实验目的、实验方法、观测指标、实验结束后处死动物的方法等:</p> <p>本次实验主要观察(±)-dactylicapnosine A 和 isocorydine 化合物的抗炎活性;方法采用二甲苯致小鼠耳廓肿胀模型,主要观察化合物对抗二甲苯所致的小鼠耳廓肿胀程度;实验结束采用气体麻醉的方法对小鼠施行安乐死。</p>			

审查依据	<p>1. 该项目是否必须用实验动物进行实验,即能否用计算机模拟、细胞培养等非生命方法替代动物或用低等动物替代高等动物进行实验;</p> <p>2. 表中所填申请人资格和所用动物的品种品系、质量等级、规格是否合适,能否通过改良设计方案或用高质量的动物来减少所用动物的数量;</p> <p>3. 能否通过改进实验方法、调整实验观测指标、改良处死动物的方法,来优化实验方案、善待动物;</p> <p>4. 保证动物福利措施是否落实。</p>
<p>动物实验伦理审查小组负责人意见:  签章 </p> <p style="text-align: right;">2018年12月11日</p>	
<p>动物管理委员会负责人意见:  签章 </p> <p style="text-align: right;">2018年12月11日</p>	
<p>主管单位负责人意见:  签章 </p> <p style="text-align: right;">2018年12月11日</p>	

说明:

1、申请部门填到室、园(库)、中心;2、申请人为课题负责人本人时则只填负责人一栏;3、联系电话填本项目申请人的电话;4、实验要点只写摘要;5、主管单位签章为所主管科研的领导签章;6、附则。6.1 本规程由中科院植物所实验动物管理委员会负责解释;6.2 本规程自发布之日起生效实施。

Reference

- (1) Wang, B.; Yang, Z. F.; Zhao, Y. L.; Liu, Y. P.; Deng, J.; Huang, W. Y.; Li, X. N.; Wang, X. H.; Luo, X. D., Anti-inflammatory isoquinoline with bis-*seco*-aporphine skeleton from *Dactylicapnos scandens*. *Org. Lett.* **2018**, *20*, 1647-1650.
- (2) Shang, J. H.; Cai, X. H.; Feng, T.; Zhao, Y. L.; Wang, J. K.; Zhang, L. Y.; Yan, M.; Luo, X. D., Pharmacological evaluation of *Alstonia scholaris*: Anti-inflammatory and analgesic effects. *Journal of Ethnopharmacology* **2010**, *129*, 174-181.
- (3) Li, Q.; Yang, K. X.; Zhao, Y. L.; Qin, X. J.; Yang, X. W.; Liu, L.; Liu, Y. P.; Luo, X. D., Potent anti-inflammatory and analgesic steroidal alkaloids from *Veratrum taliense*. *Journal of Ethnopharmacology*

2016, 179, 274-279.

- (4) Mishra, D.; Ghosh, G.; Kumar, P. S.; Panda, P. K., An experimental study of analgesic activity of selective COX-2 inhibitor with conventional NSAIDs. *Asian J. Pharm. Clin. Res.* **2011**, 4, 78–81.
- (5) Hunskaar, S.; Fasmer, O. B.; Hole, K., Formalin test in mice, a useful technique for evaluating mild analgesics. *J. Neurosci. Methods* **1985**, 14, 69–76.
- (6) Hunskaar, S.; Hole, K., The formalin test in mice: dissociation between inflammatory and non-inflammatory pain. *Pain physician* **1987**, 30, 103–114.
- (7) Eddy, N. B.; Leimbach, D., Synthetic analgesics. II. Dithienylbutenyl- and dithienylbutylamines. *J. Pharmacol. Exp. Ther.* **1953**, 107, 385–393.
- (8) Kim, H. D.; Cho, H. R.; Moon, S. B.; Shin, H. D.; Yang, K. J.; Park, B. R.; Jang, H. J.; Kim, L. S.; Lee, H. S.; Ku, S. K., Effects of *b*-Glucan from *Aureobasidium pullulans* on Acute Inflammation in Mice. *Arch. Pharm. Res.* **2007**, 30, 323-328.
- (9) Dewanjee, S.; Maiti, A.; Sahu, R.; Dua, T. K.; Mandal, S. C., Study of anti-inflammatory and antinociceptive activity of hydroalcoholic extract of *Schima wallichii* bark. *Pharm. Biol.* **2009**, 47, 402-407.
- (10) Lee, I. O.; Jeong, Y. S., Effects of Different Concentrations of Formalin on Paw Edema and Pain Behaviors in Rats. *J. Korean. Med. Sci.* **2002**, 17, 81-85.
- (11) García, M. D.; Fernández, M. A.; Alvarez, A.; T., S. M., Antinociceptive and anti-inflammatory effect of the aqueous extract from leaves of *Pimenta racemosa* var. *ozua* (Mirtaceae). *Journal of Ethnopharmacology* **2004**, 91, 69-73.

7. Supplementary Figures

Figure S01. The HPLC profiles of separation of (+)-1 and (-)-1.

Chromatogram condition: Reprosil chiral-AM, 5 μ m, 250mm*4.6mm r65am. S2546 (Dr. maisch), n-hexane: ethanol= 80:20 as mobile phase.

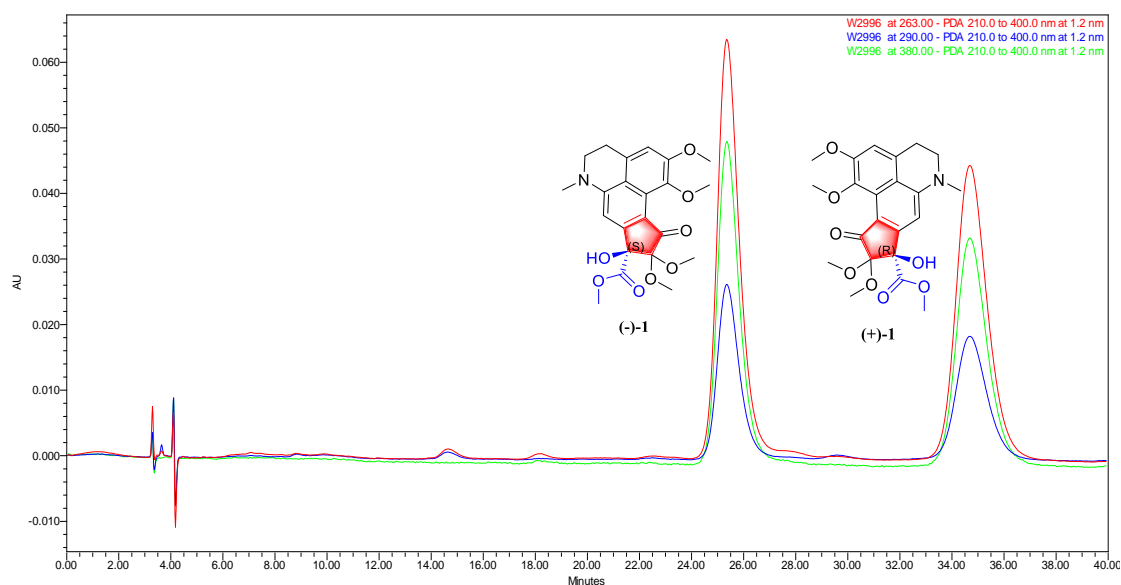


Figure S02. The HPLC profiles of separation of (+)-**2** and (-)-**2**.

Chromatogram condition: Reprosil chiral-AM, 5 μ m, 250mm*4.6mm r65am. S2546 (Dr. maisch),
n-hexane: ethanol= 70:30 as mobile phase.

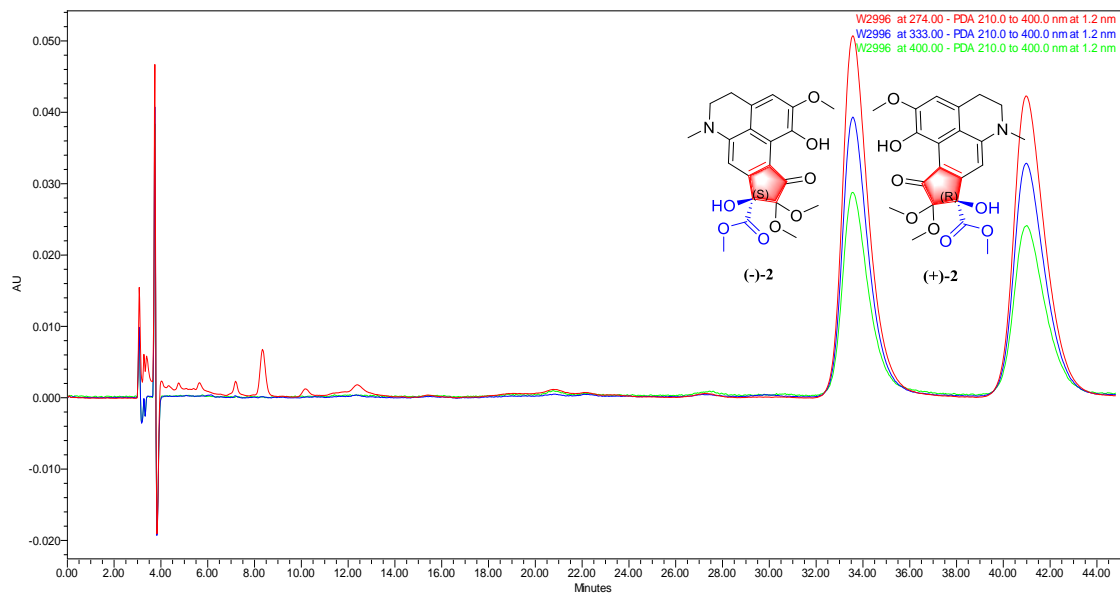


Figure S03. The overlapped experimental CD spectra of compounds (+)-**2** and (-)-**2**.

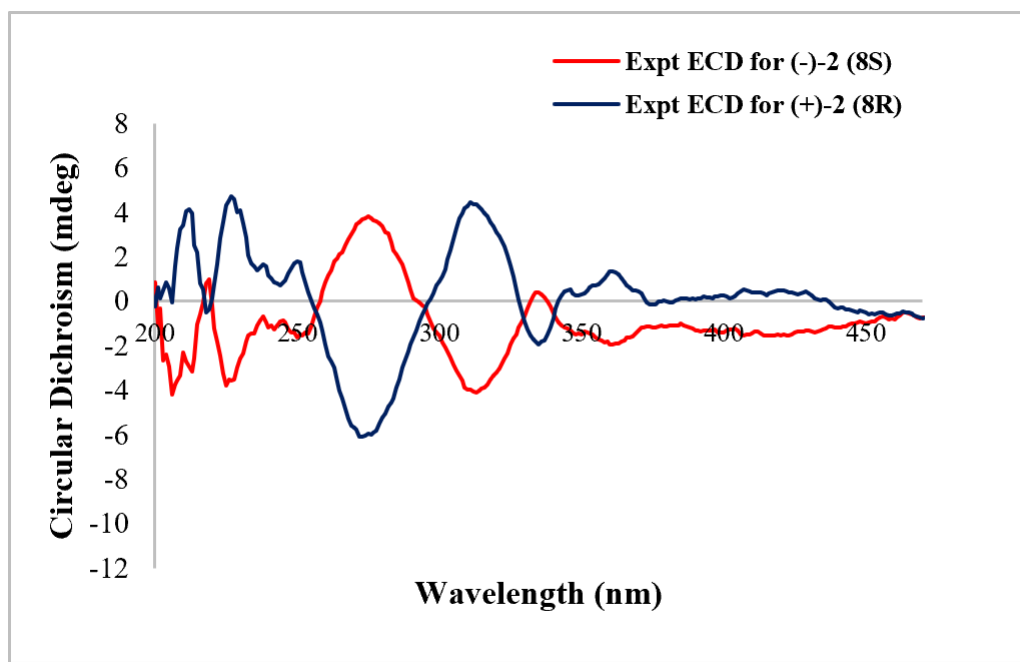


Figure S04. ^1H NMR spectrum of compound **1** ($\text{CDCl}_3/\text{CD}_3\text{OD}$)

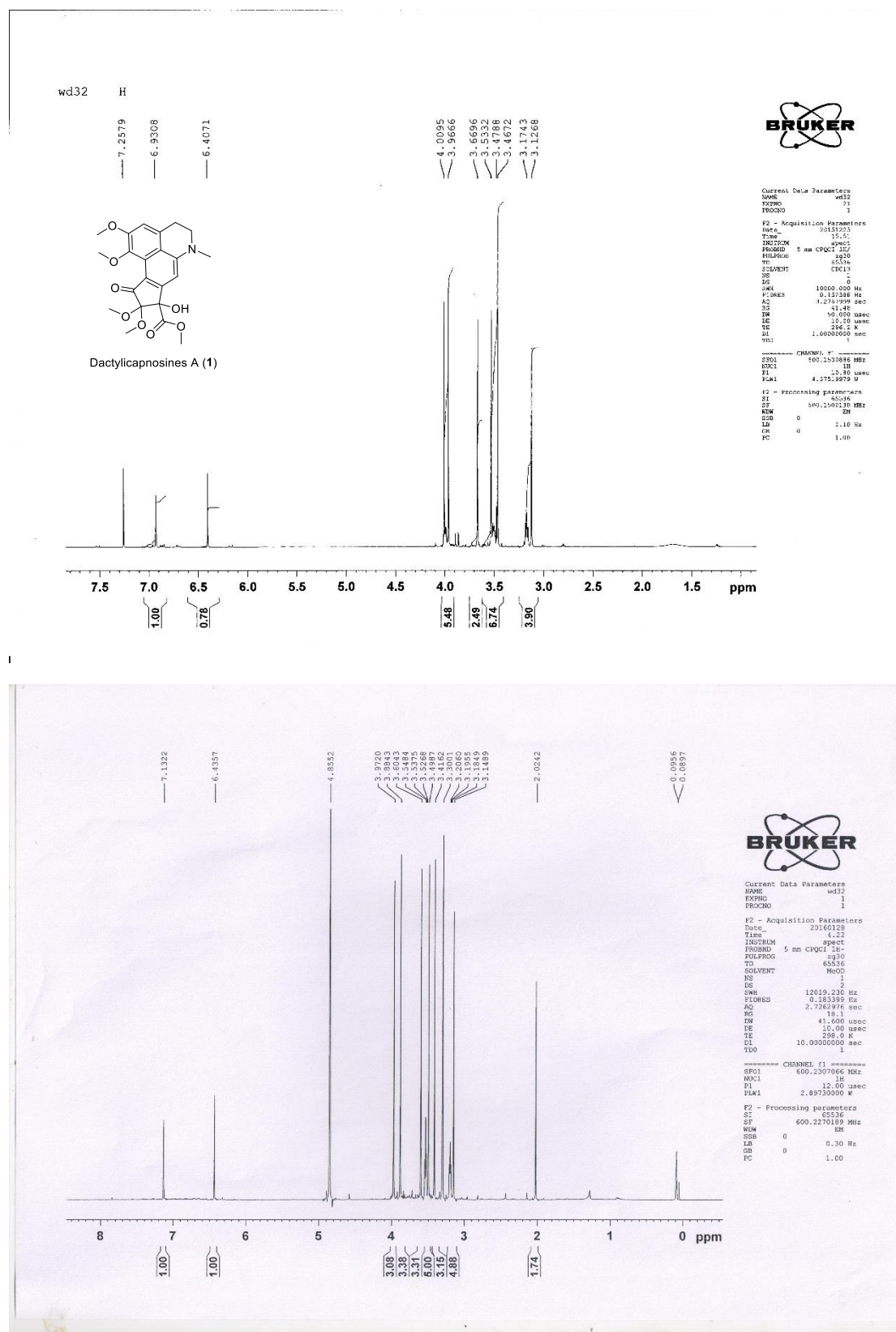
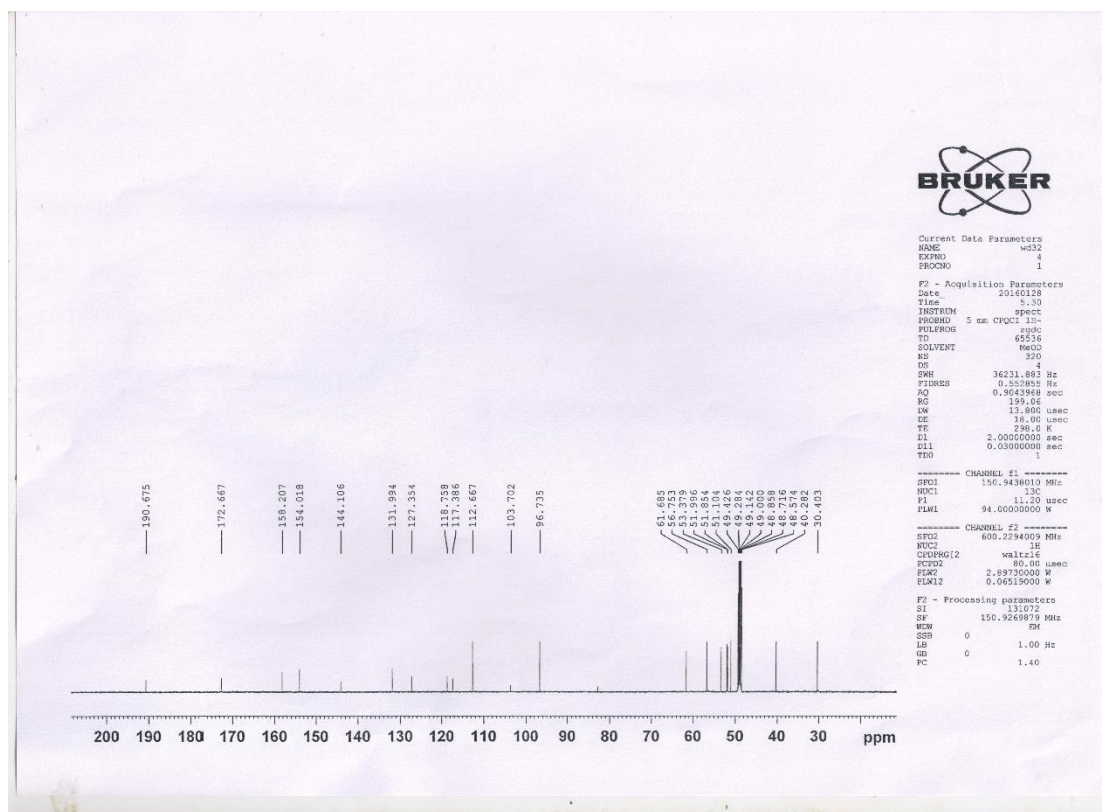
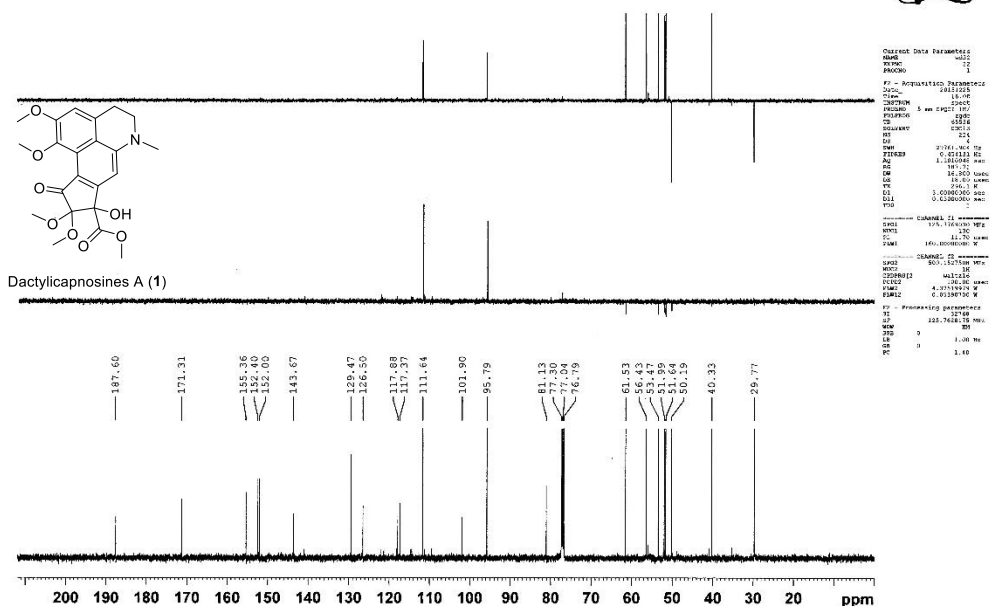


Figure S05. ^{13}C NMR and DEPT spectra of compound **1** ($\text{CDCl}_3/\text{CD}_3\text{OD}$)

wd32 c13 and dept



Dactylicapnosines A (1)

CN1Cc2cc3c(c1)c(OC)c(OC)c3C(=O)c4c2OC(=O)O4

1D 13C NMR (400 MHz, CDCl₃)

Chemical Shift (ppm)	Assignment
158.0	C-1
157.5	C-2
157.0	C-3
156.5	C-4
156.0	C-5
155.5	C-6
155.0	C-7
154.5	C-8
154.0	C-9
153.5	C-10
153.0	C-11
152.5	C-12
152.0	C-13
151.5	C-14
151.0	C-15
150.5	C-16
150.0	C-17
149.5	C-18
149.0	C-19
148.5	C-20
148.0	C-21
147.5	C-22
147.0	C-23
146.5	C-24
146.0	C-25
145.5	C-26
145.0	C-27
144.5	C-28
144.0	C-29
143.5	C-30
143.0	C-31
142.5	C-32
142.0	C-33
141.5	C-34
141.0	C-35
140.5	C-36
140.0	C-37
139.5	C-38
139.0	C-39
138.5	C-40
138.0	C-41
137.5	C-42
137.0	C-43
136.5	C-44
136.0	C-45
135.5	C-46
135.0	C-47
134.5	C-48
134.0	C-49
133.5	C-50
133.0	C-51
132.5	C-52
132.0	C-53
131.5	C-54
131.0	C-55
130.5	C-56
130.0	C-57
129.5	C-58
129.0	C-59
128.5	C-60
128.0	C-61
127.5	C-62
127.0	C-63
126.5	C-64
126.0	C-65
125.5	C-66
125.0	C-67
124.5	C-68
124.0	C-69
123.5	C-70
123.0	C-71
122.5	C-72
122.0	C-73
121.5	C-74
121.0	C-75
120.5	C-76
120.0	C-77
119.5	C-78
119.0	C-79
118.5	C-80
118.0	C-81
117.5	C-82
117.0	C-83
116.5	C-84
116.0	C-85
115.5	C-86
115.0	C-87
114.5	C-88
114.0	C-89
113.5	C-90
113.0	C-91
112.5	C-92
112.0	C-93
111.5	C-94
111.0	C-95
110.5	C-96
110.0	C-97
109.5	C-98
109.0	C-99
108.5	C-100
108.0	C-101
107.5	C-102
107.0	C-103
106.5	C-104
106.0	C-105
105.5	C-106
105.0	C-107
104.5	C-108
104.0	C-109
103.5	C-110
103.0	C-111
102.5	C-112
102.0	C-113
101.5	C-114
101.0	C-115
100.5	C-116
100.0	C-117
99.5	C-118
99.0	C-119
98.5	C-120
98.0	C-121
97.5	C-122
97.0	C-123
96.5	C-124
96.0	C-125
95.5	C-126
95.0	C-127
94.5	C-128
94.0	C-129
93.5	C-130
93.0	C-131
92.5	C-132
92.0	C-133
91.5	C-134
91.0	C-135
90.5	C-136
90.0	C-137
89.5	C-138
89.0	C-139
88.5	C-140
88.0	C-141
87.5	C-142
87.0	C-143
86.5	C-144
86.0	C-145
85.5	C-146
85.0	C-147
84.5	C-148
84.0	C-149
83.5	C-150
83.0	C-151
82.5	C-152
82.0	C-153
81.5	C-154
81.0	C-155
80.5	C-156
80.0	C-157
79.5	C-158
79.0	C-159
78.5	C-160
78.0	C-161
77.5	C-162
77.0	C-163
76.5	C-164
76.0	C-165
75.5	C-166
75.0	C-167
74.5	C-168
74.0	C-169
73.5	C-170
73.0	C-171

Figure S07. HMBC spectrum of compound **1** (CD₃OD)

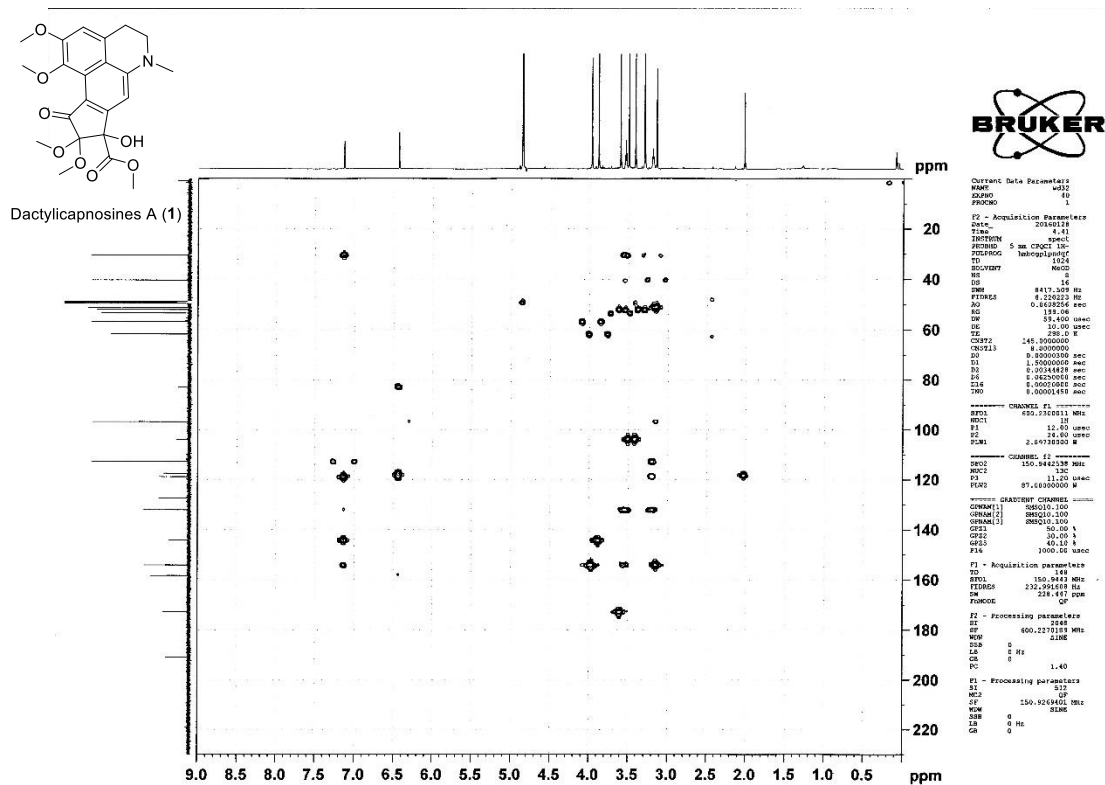


Figure S08. HREIMS spectrum of compound **1**

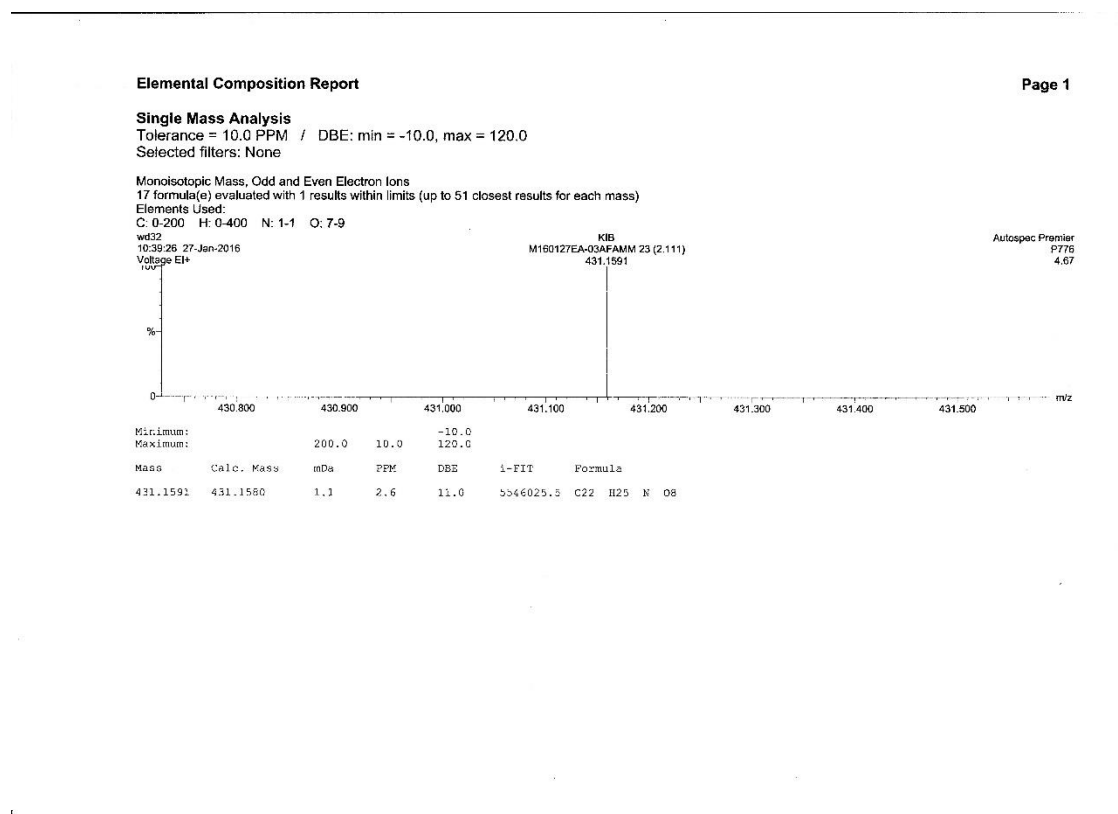


Figure S09. ESIMS spectrum of compound 1

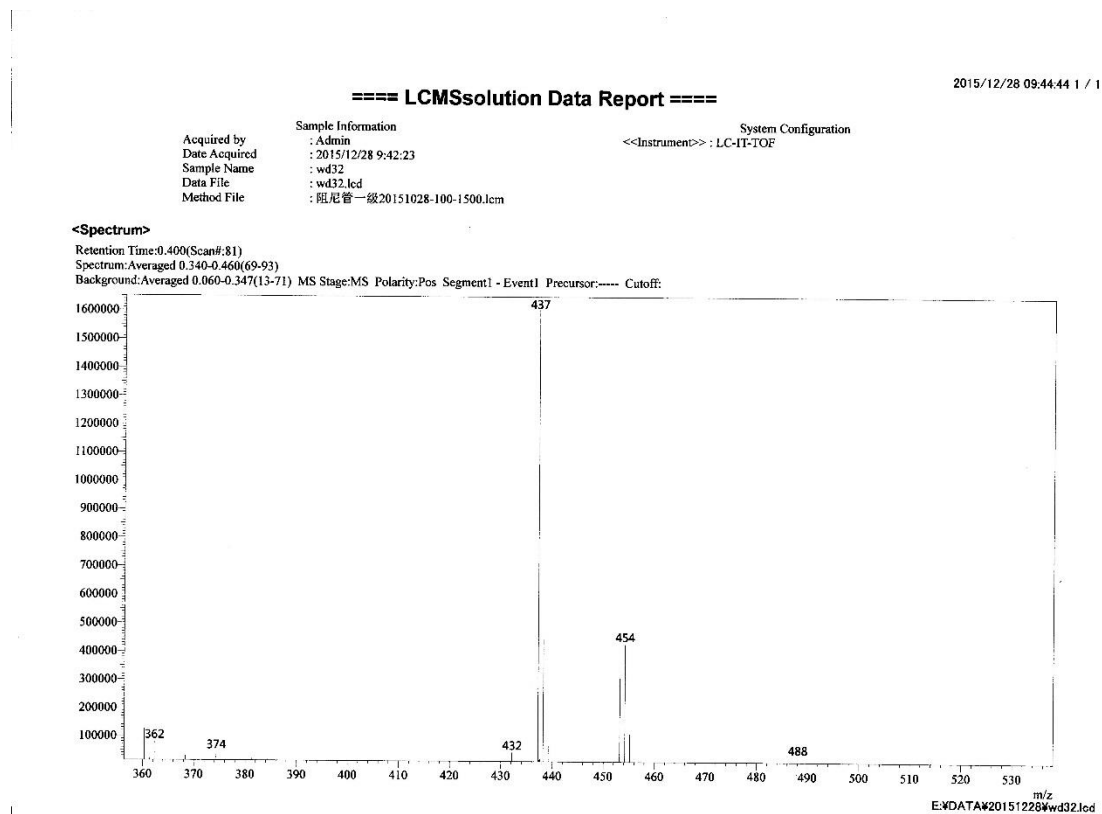
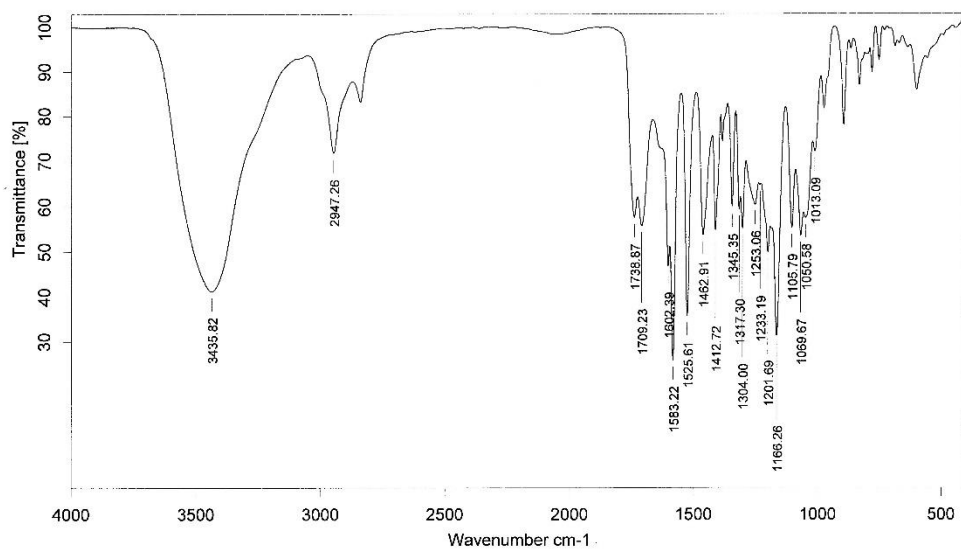


Figure S10. IR spectrum of compound **1**



Sample : wd32	Frequency Range : 399.246 - 3996.32	Measured on : 25/01/2016
Technique : KBr压片	Resolution : 4	Instrument : Tensor27
Customer : 160201IR2	Zerofilling : 2	Sample Scans : 16
	Acquisition : Double Sided, For	

Figure S11. UV spectrum of compound **1**

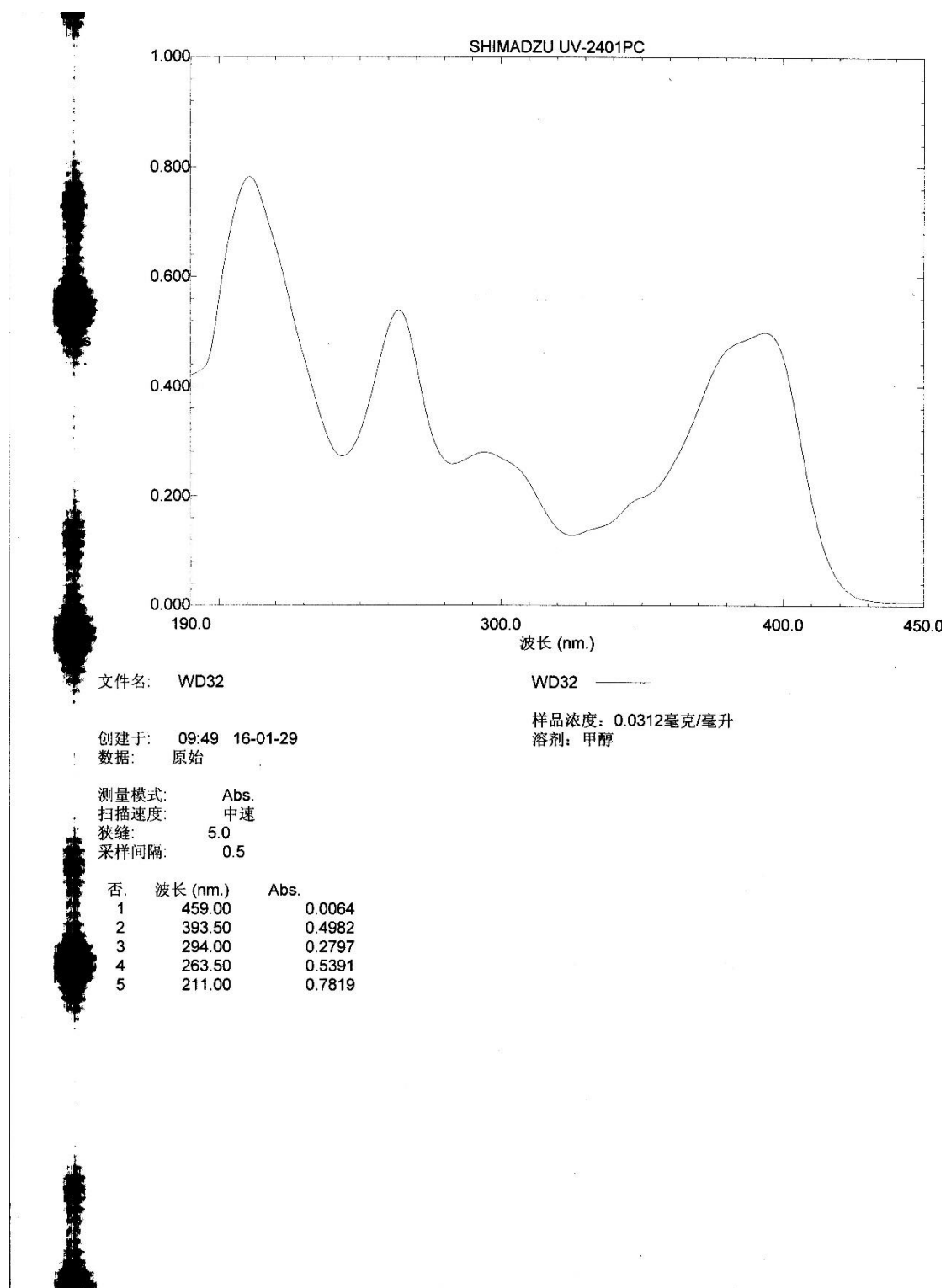
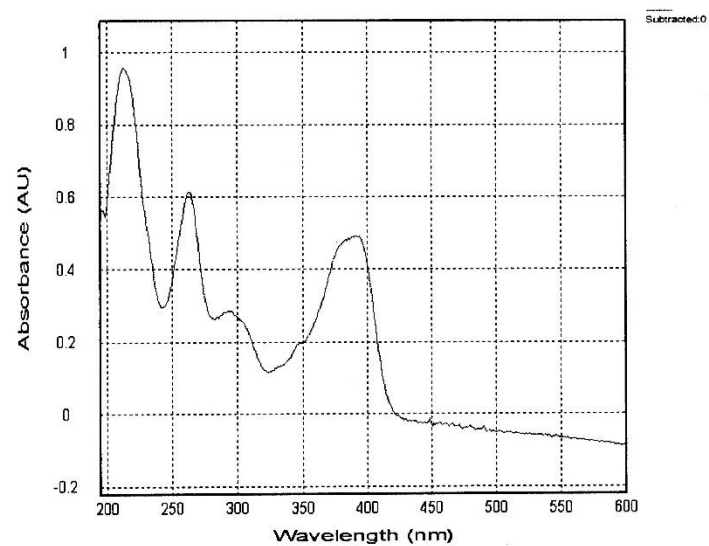
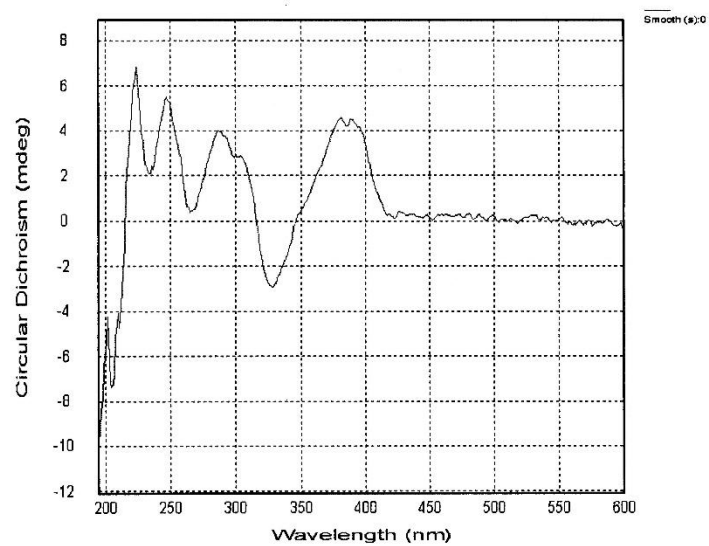


Figure S12. CD spectrum of compound (+)-1

WD32B



File: CD WD32B-1mm(195-600)16041415.dsx

ProBinaryX

Attributes :

- Time Stamp :Thu Apr 14 18:53:32 2016

- File ID : {5041B49F-5661-494f-A9F9-0DF0EA0E8FE3}

- Is CFR Compliant : false

- Original unaltered data

Remarks:

- HV (CDDC channel): 0 v

- Time per point: 1 s

- Description: Sample 1

- Concentration: 0.2000mg/mL MeOH

- Pathlength: 1 mm

Settings:

- Time-per-point: 1s (25us x 40000)

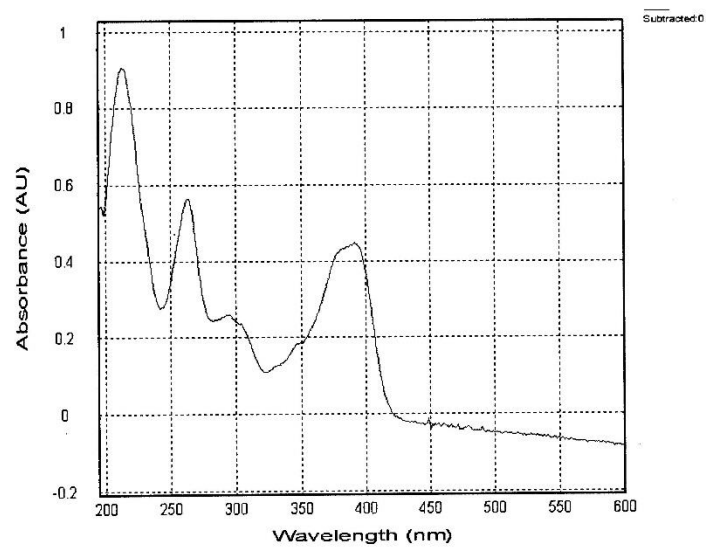
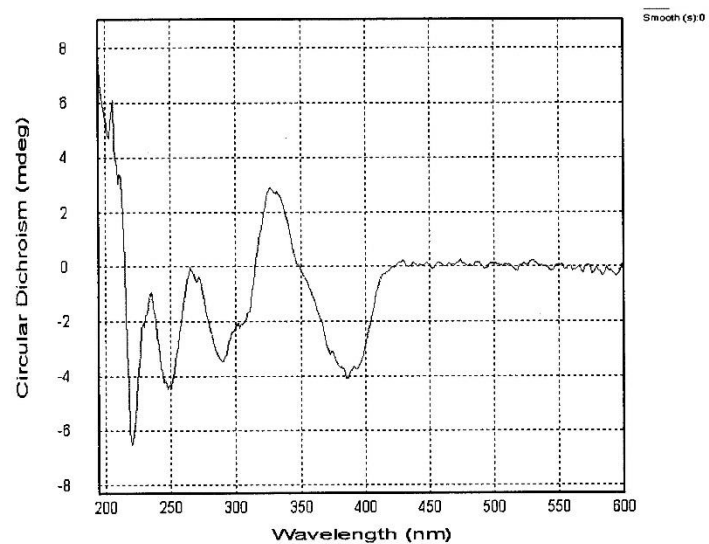
- Wavelength: 195nm - 600nm

- Step Size: 1nm

- Bandwidth: 1nm

Figure S13. CD spectrum of compound (-)-1

WD32A



File: CD WD32A-1mm(195-600)16041414.dsx

ProBinaryX

Attributes :

- Time Stamp :Thu Apr 14 18:42:39 2016

- File ID : {5822A986-1FE7-46eb-B6DA-85D3F35E2B6A}

- Is CFR Compliant : false

- Original unaltered data

Remarks:

- HV (CDDC channel): 0 v

- Time per point: 1 s

- Description: Sample 1

- Concentration: 0.2000mg/mL MeOH

- Pathlength: 1 mm

Settings:

- Time-per-point: 1s (25us x 40000)

- Wavelength: 195nm - 600nm

- Step Size: 1nm

- Bandwidth: 1nm

Figure S14. ^1H NMR spectrum of compound **2** (CDCl_3)

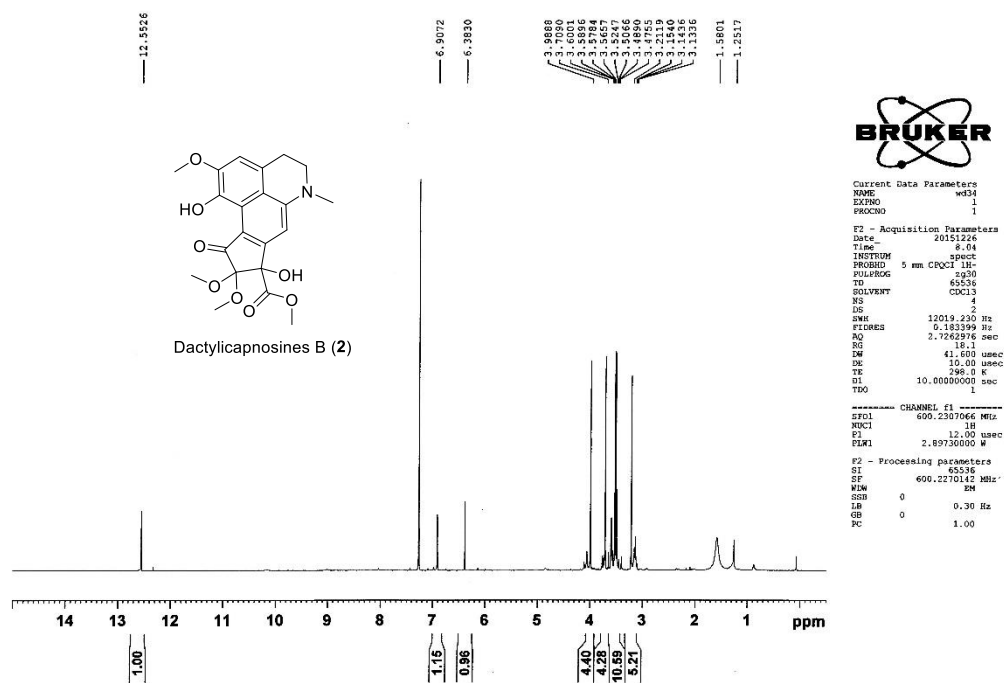
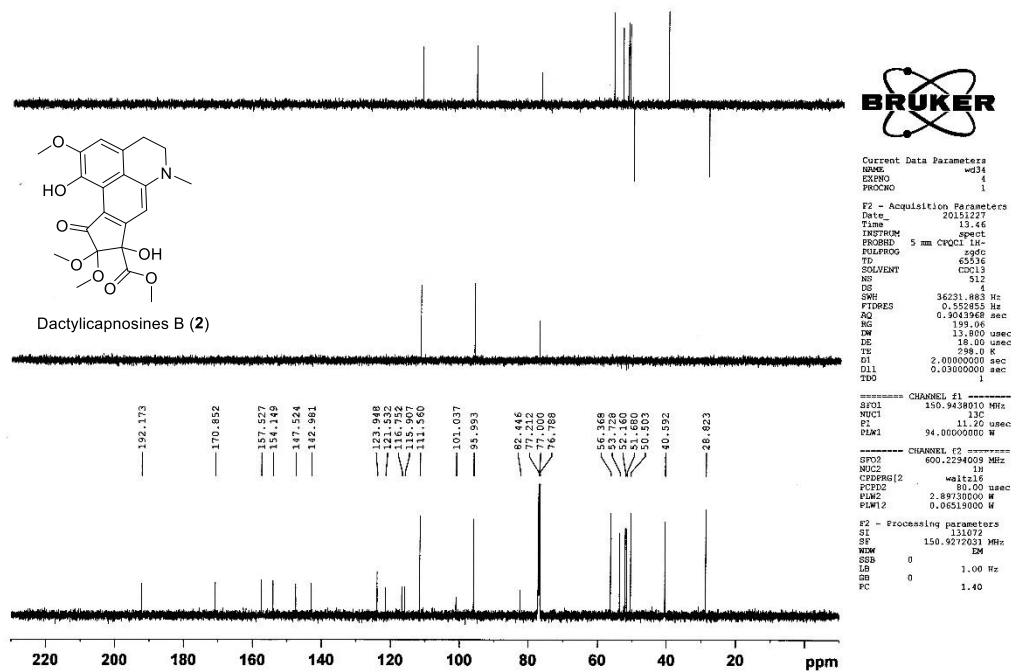


Figure S15. ^{13}C NMR and DEPT spectra of compound **2** (CDCl_3)



1

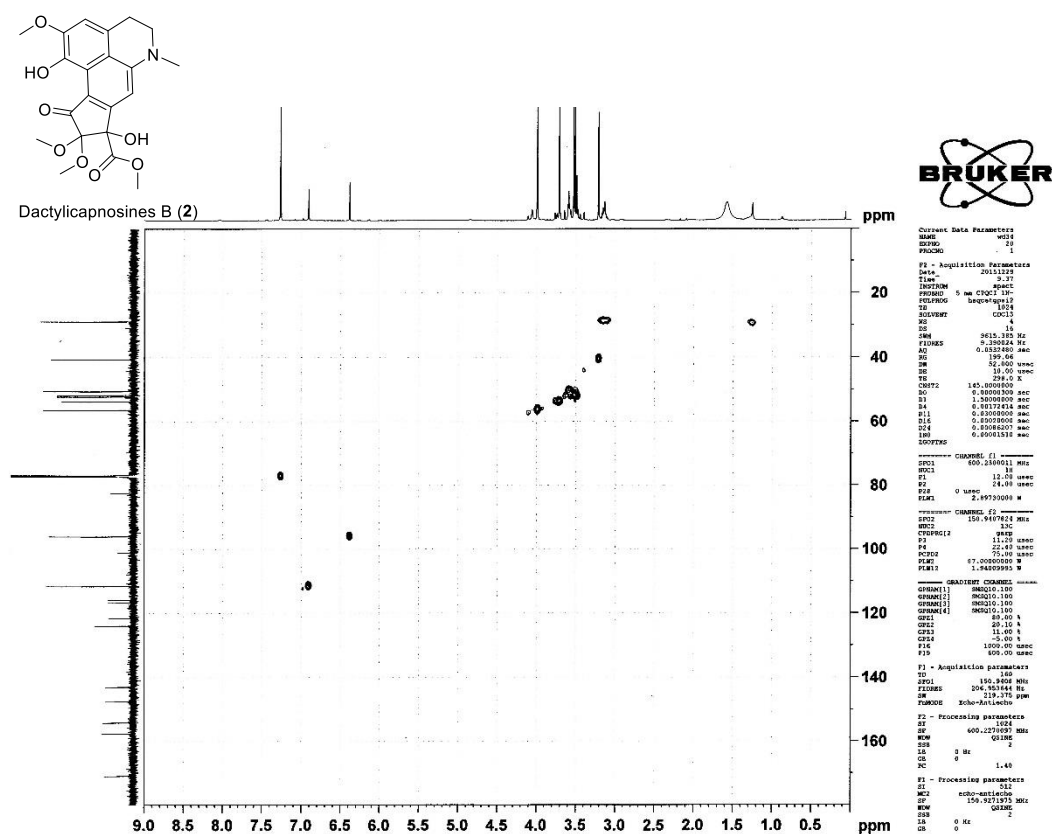


Figure S17. HMBC spectrum of compound 2 (CDCl₃)

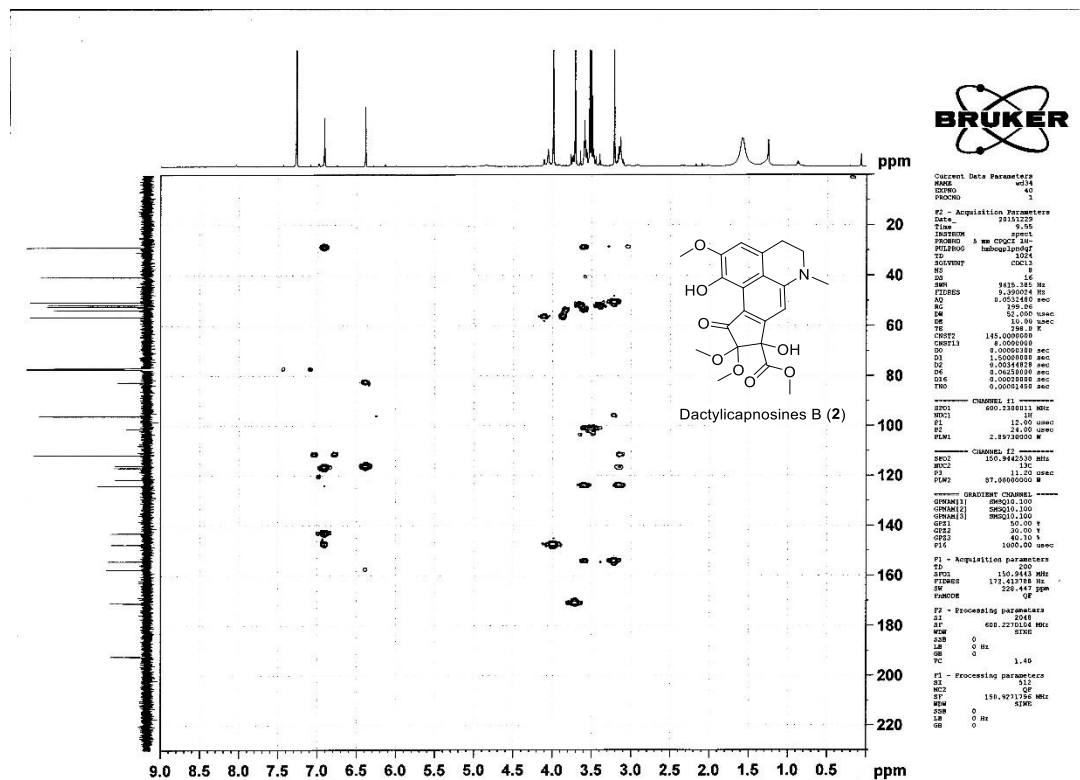


Figure S18. HREIMS spectrum of compound **2**

Elemental Composition Report

Page 1

Single Mass Analysis (displaying only valid results)

Tolerance = 10.0 PPM / DBE: min = -1.5, max = 50.0

Selected filters: None

Monoisotopic Mass, Odd and Even Electron Ions

14 formula(e) evaluated with 1 results within limits (up to 50 closest results for each mass)

Elements Used:

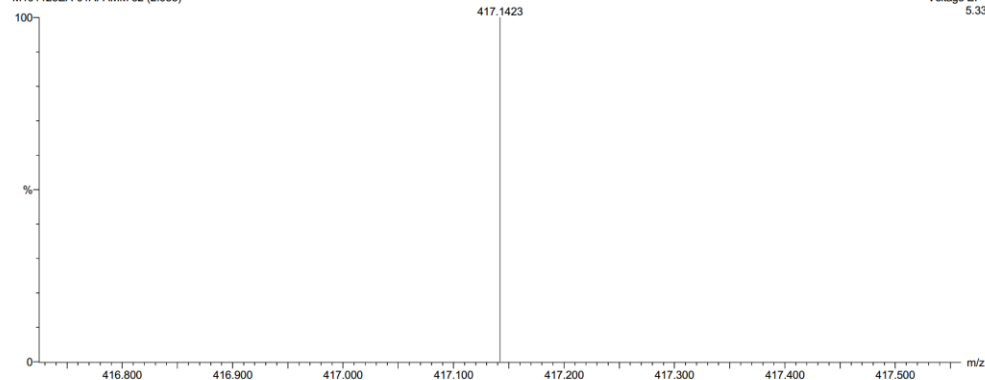
C: 0-200 H: 0-400 N: 1-1 O: 7-9

wd-34

M191125EA-01AFAMM 32 (2.938)

25-Nov-2019 13:47:23

Autospec
Voltage EI+
5.33



Minimum:						
Maximum:	500.0	10.0		-1.5		
				50.0		
Mass	Calc. Mass	mDa	PPM	DBE	i-FIT	Formula
417.1423	417.1424	-0.1	-0.2	11.0	5546025.5	C21 H23 N O8

Figure S19. ESIMS spectrum of compound 2

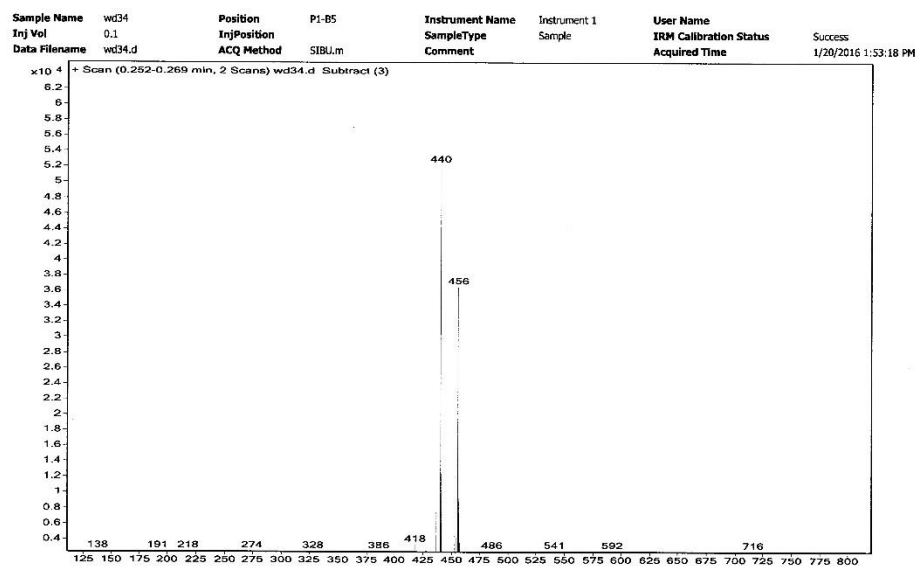
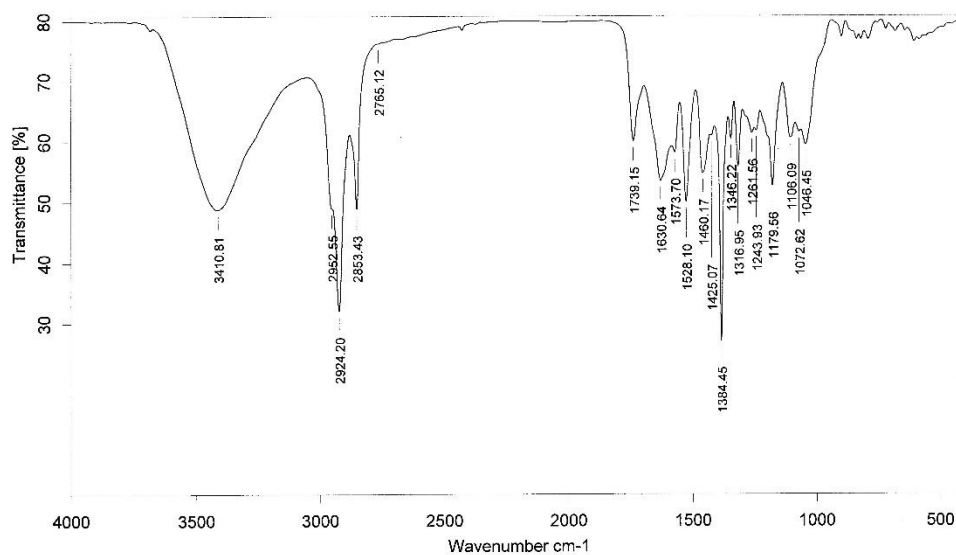


Figure S20. IR spectrum of compound **2**



Sample : wd34		Frequency Range : 399.246 - 3996.32		Measured on : 25/01/2016	
Technique : KBr压片	Resolution : 4	Instrument : Tensor27		Sample Scans : 16	
Customer : 160201IR3	Zerofilling : 2	Acquisition : Double Sided, For			

Figure S21. UV spectrum of compound 2

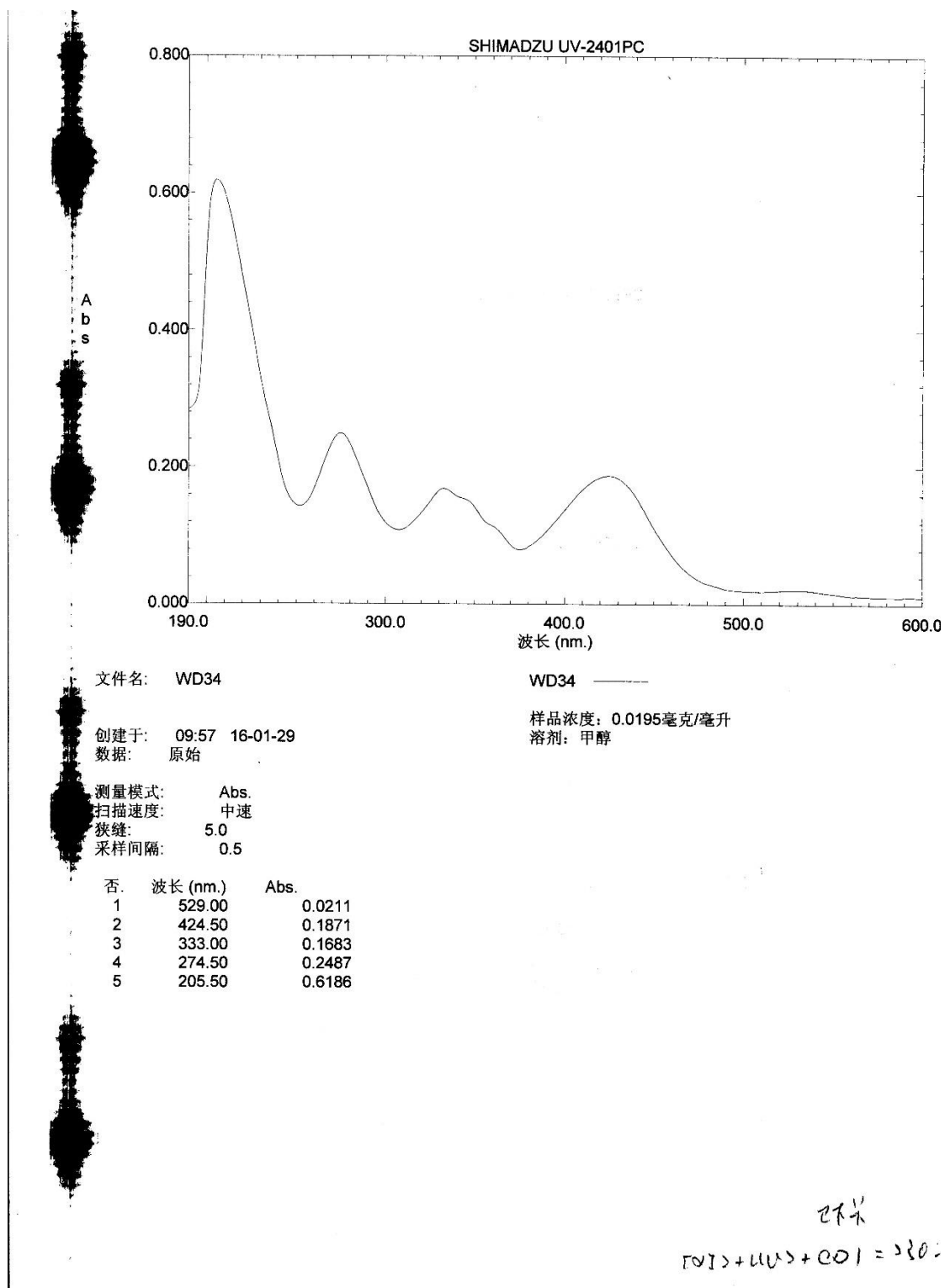
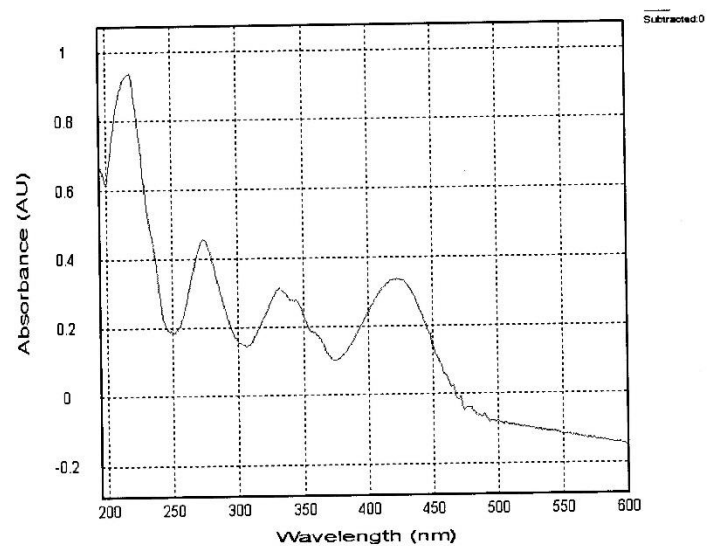
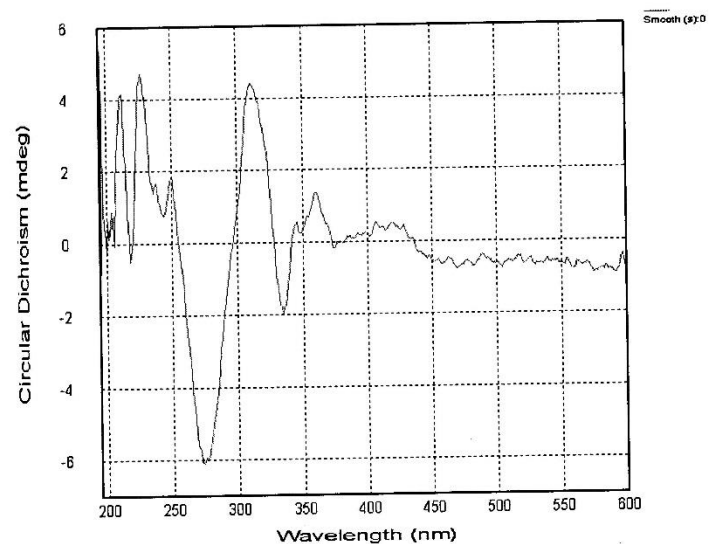


Figure S22. CD spectrum of compound (+)-2

WD34B



File: CD WD34B-1mm(195-600)16041909.dsx

ProBinaryX

Attributes :

- Time Stamp :Tue Apr 19 19:08:25 2016

- File ID : {184D3ECE-8820-4651-B469-727BD7A6F198}

- Is CFR Compliant : false

- Original unaltered data

Remarks:

- HV (CDDC channel): 0 v

- Time per point: 1 s

- Description: Sample 1

- Concentration: 0.2800mg/mL MeOH

- Pathlength: 1 mm

Settings:

- Time-per-point: 1s (25us x 40000)

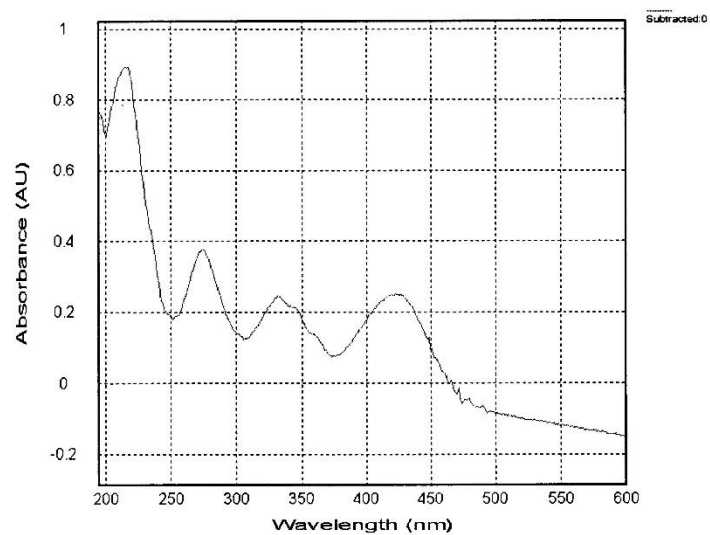
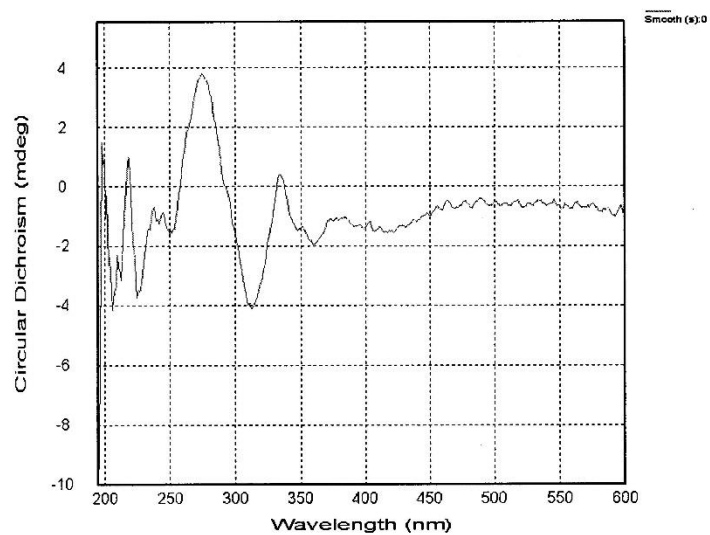
- Wavelength: 195nm - 600nm

- Step Size: 1nm

- Bandwidth: 1nm

Figure S23. CD spectrum of compound (-)-2

WD34A



File: CD WD34A-1mm(195-600)16041910.dsx

ProBinaryX

Attributes :

- Time Stamp :Tue Apr 19 19:19:20 2016

- File ID : {06ABF8E0-F8C9-4217-A0F6-017379DA01A1}

- Is CFR Compliant : false

- Original unaltered data

Remarks:

- HV (CDDC channel): 0 v

- Time per point: 1 s

- Description: Sample 1

- Concentration: 0.2760mg/mL MeOH

- Pathlength: 1 mm

Settings:

- Time-per-point: 1s (25us x 40000)

- Wavelength: 195nm - 600nm

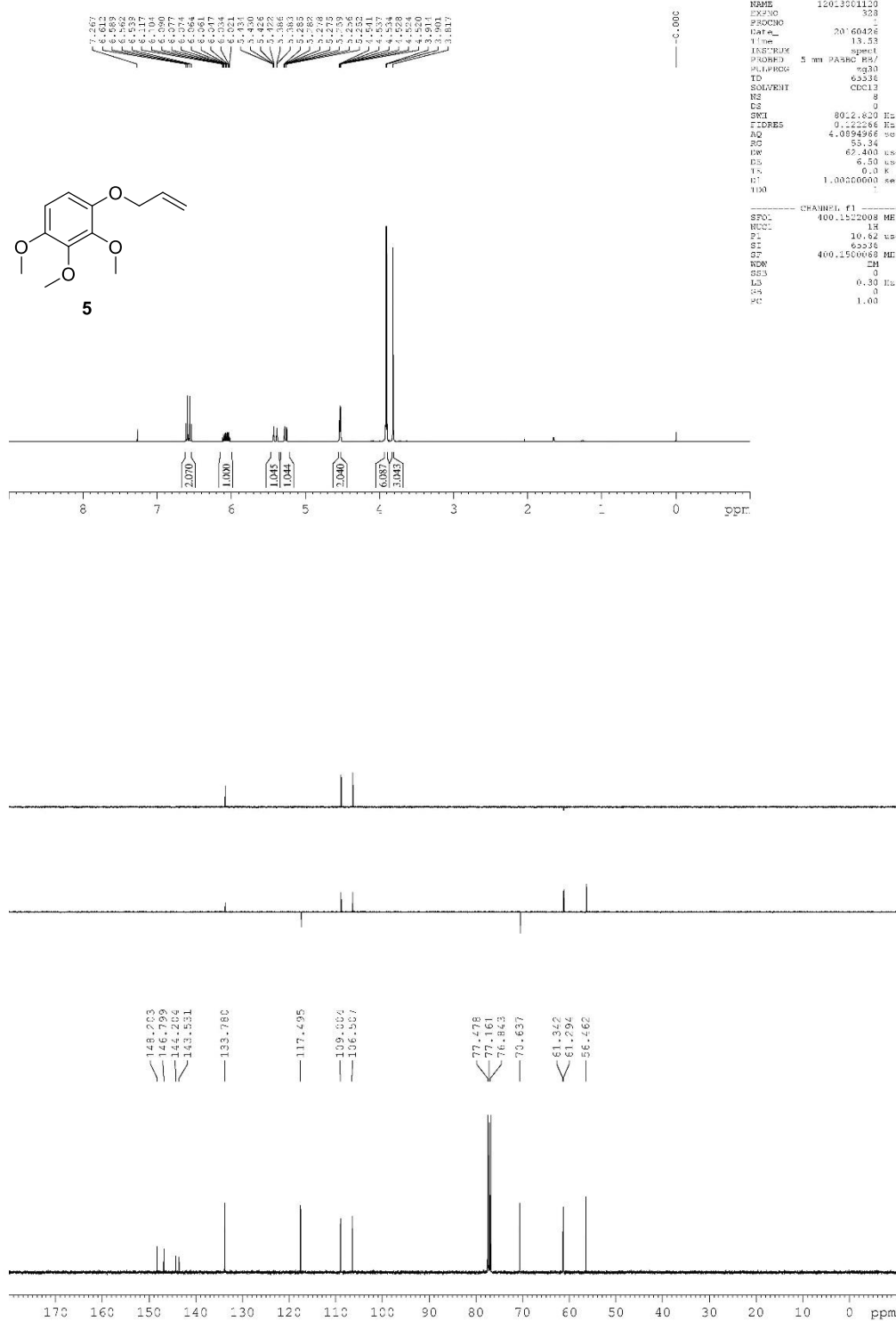
- Step Size: 1nm

- Bandwidth: 1nm

Figure S24. Copies of NMR spectra of compounds in Total synthesis



20160430



5a

1H NMR (400 MHz, CDCl₃)

Chemical shift (ppm): 7.562, 6.432, 6.036, 6.020, 5.994, 5.977, 5.961, 5.932, 5.916, 5.420, 5.411, 5.407, 5.382, 5.374, 5.369, 5.357, 5.054, 3.953, 3.931, 3.901, 3.867, 3.831, -0.000.

Integration: 1.081, 1.012, 1.000, 2.080, 1.042, 1.046, 1.093, 2.072.

13C NMR (400 MHz, CDCl₃)

Chemical shift (ppm): 146.420, 143.975, 143.493, 140.278, 136.718, 120.115, 115.740, 108.657, 77.479, 77.161, 76.844, 61.350, 61.053, 56.738, 34.368.

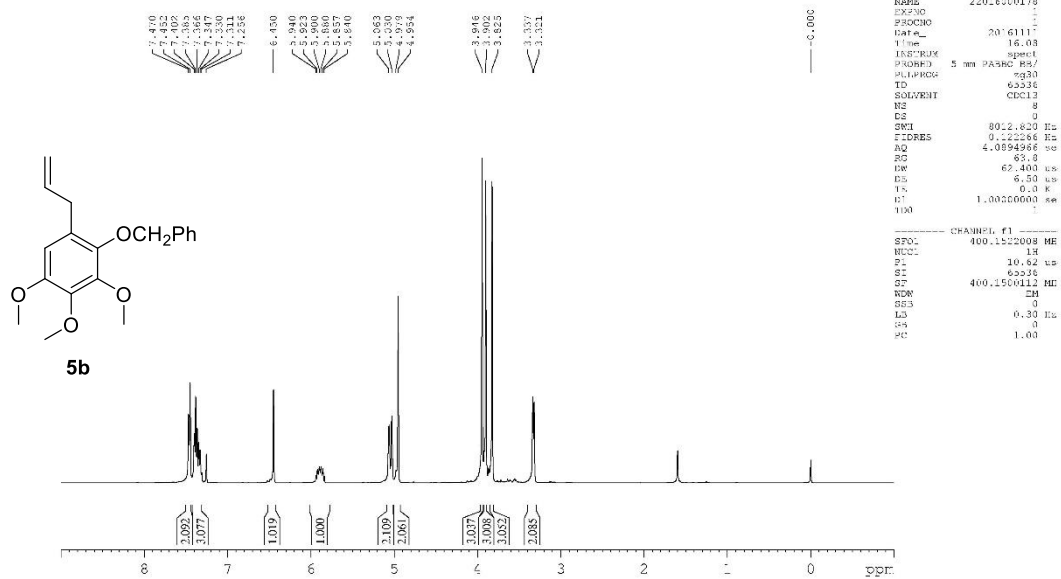
Mass Spectrometry (ESI-MS)

m/z: 201.04497 (M⁺), 203.04697 (M⁺+H₂O), 401.094966 (M⁺), 403.096966 (M⁺+H₂O).

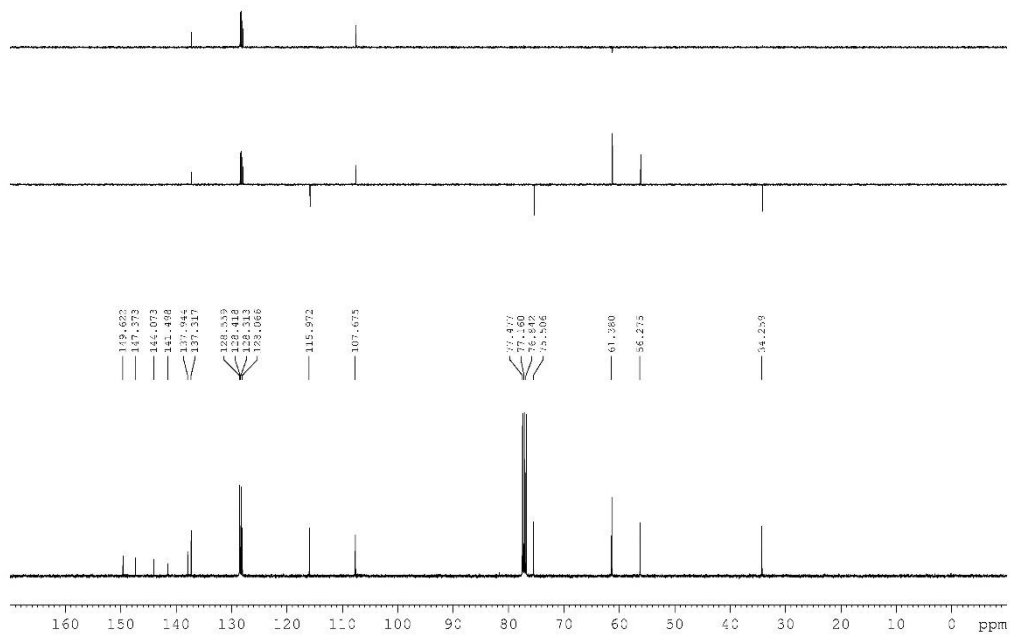
Elemental Analysis

Calcd for C₁₁H₁₂O₅: C, 55.34%; H, 4.93%; O, 39.73%. Found: C, 55.34%; H, 4.93%; O, 39.73%.

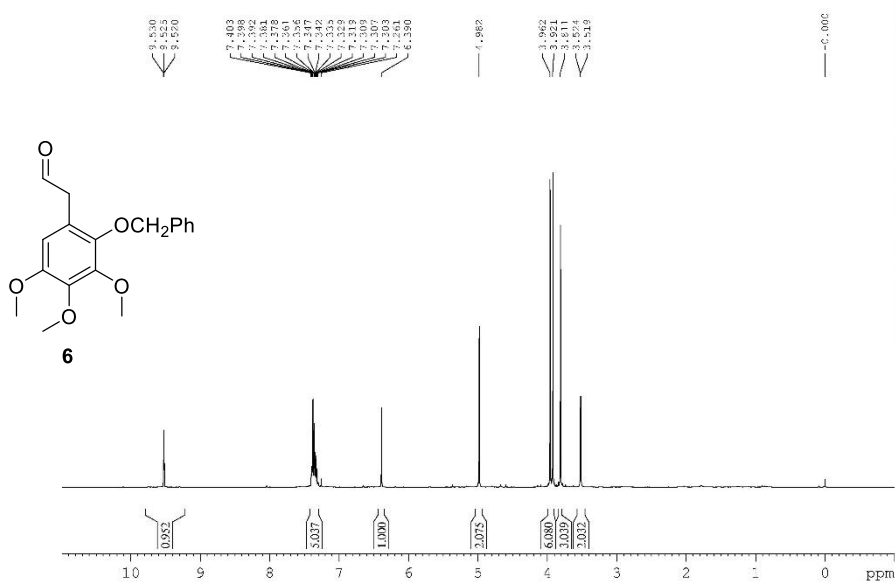
20161213



20161213



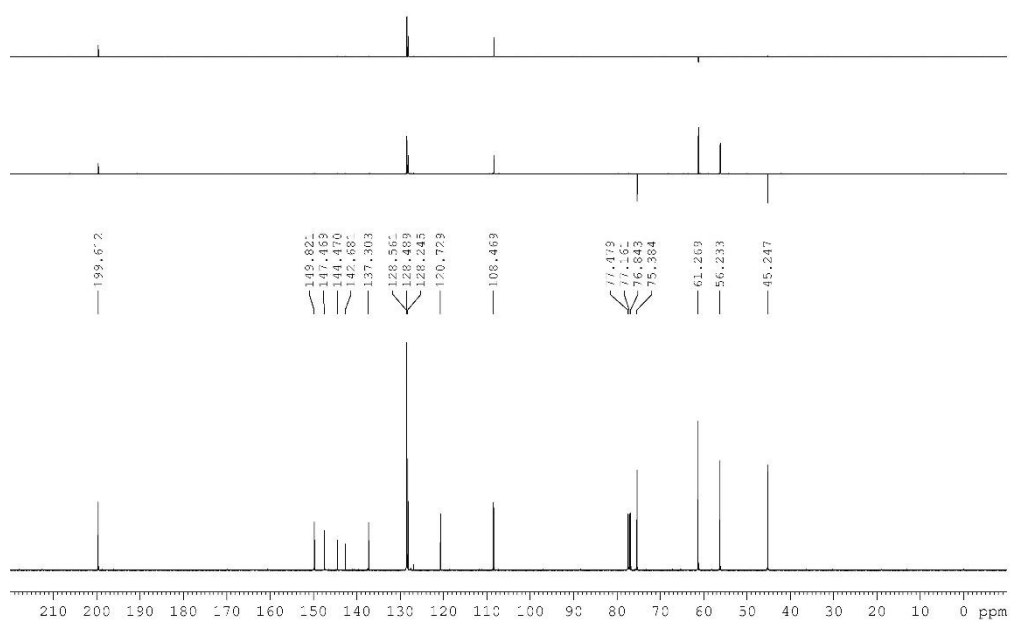
20160726



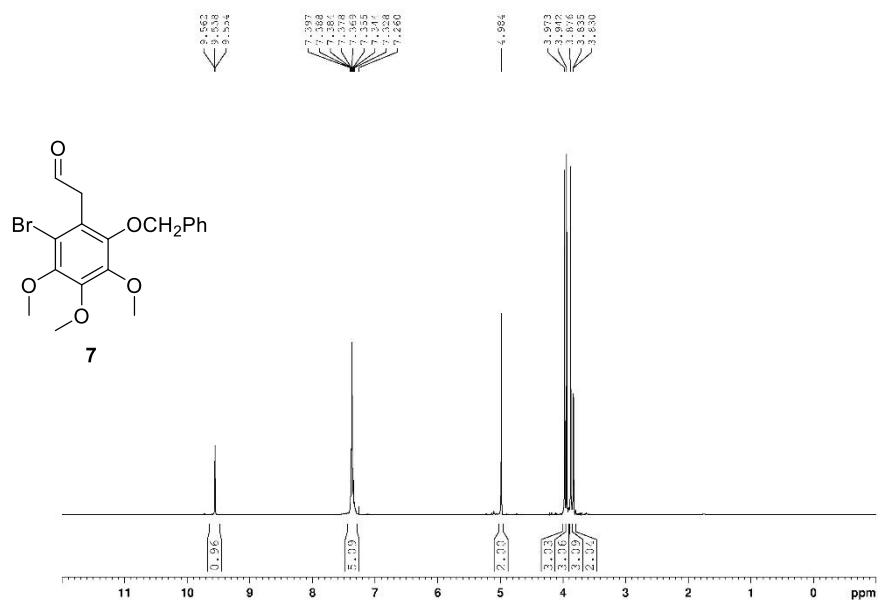
NAME 12013001120
EXPNO 323
PROCNO 1
DATA_ 70160713
F1 7.15
INSTRUM spect
PULPROG 5 mm PABPC PG/2
TD 65536
SOLVENT CDCl₃
NS 9
DS 8022.620 Hz
SWH 0.122266 Hz
FIDRES 4.0894966 us
AQ 15.56
RG 62.400 us
DS 6.50 us
TS 0.3 K
U? 1.00200000 sw
100

----- CHANNEL f1 -----
SFO: 400.1522008 MHz
NUC1: 13
P1: 10.62 us
SFO: 400.1510002 MHz
NUC2: 1H
DS: 0.30 Hz
SFO: 0
PC: 1.00

20160726



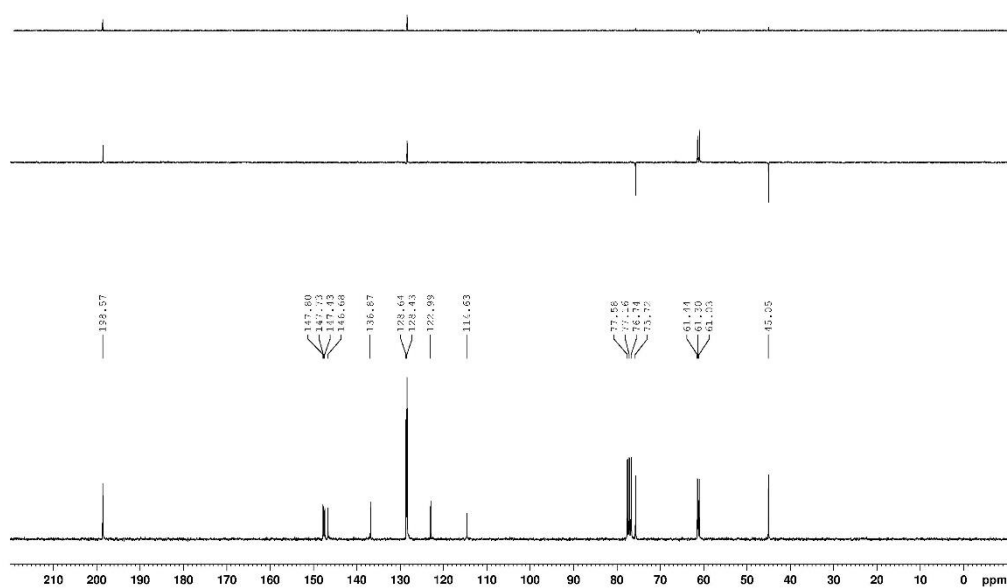
ZYJ-7-BRQUAN



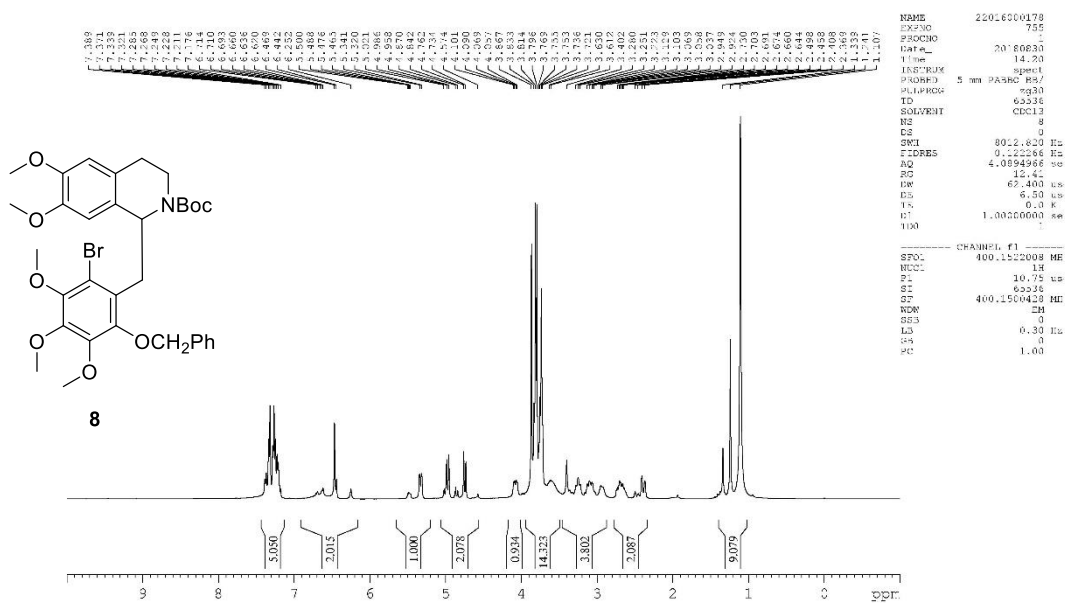
```

NAME      12013001120
EXPNO     1053
PROCNO    1
F2ACQNO   30180824
Date_     10.21
Time      09.30
INSTRUM    av300
PULPROG    zg30
RG         63555
NUC1       13
SOLVENT    CDCl3
HS         8
HC         0
SFO        6172.833 Hz
FIDRES     0.394190 Hz
AQ         5.13084660 sec
RG         90.5
UA         81.900 tsec
DS         6.30 tsec
TE         297.5 K
D1         1.22200000 sec
D10        1
===== CHANNEL f1 =====
NUC1       13
P1         7.95 tsec
PL1        -2.00 dB
PC1        305.1318534 MHz
ST         22768
SF         300.1300118 MHz
RG         0
SSB        0
LB         0.30 Hz
GB         0
PC         1.00
  
```

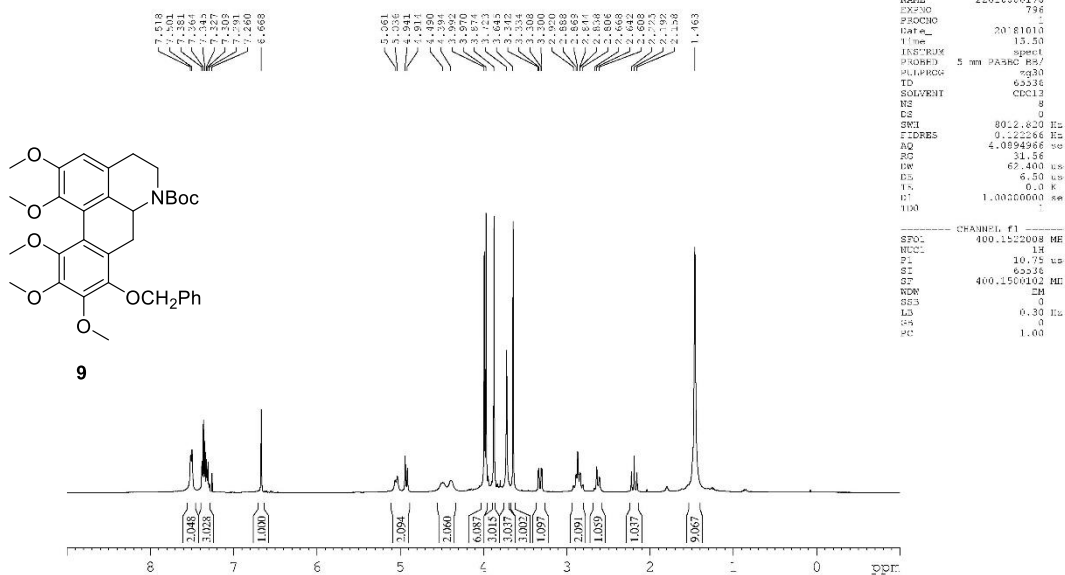
ZYJ-7-BRQUAN



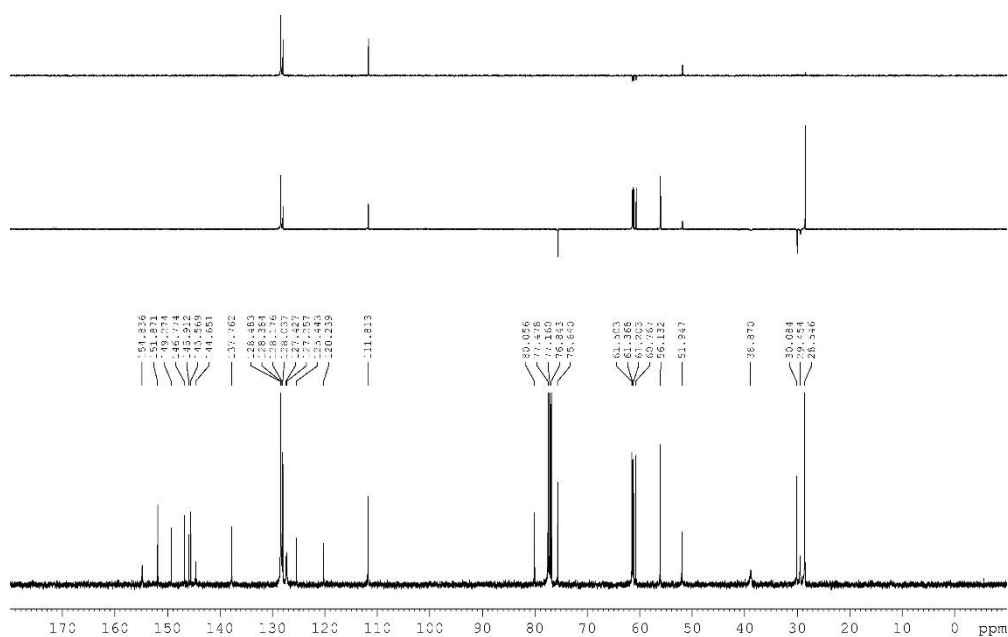
zyj-8-weiguanhuan



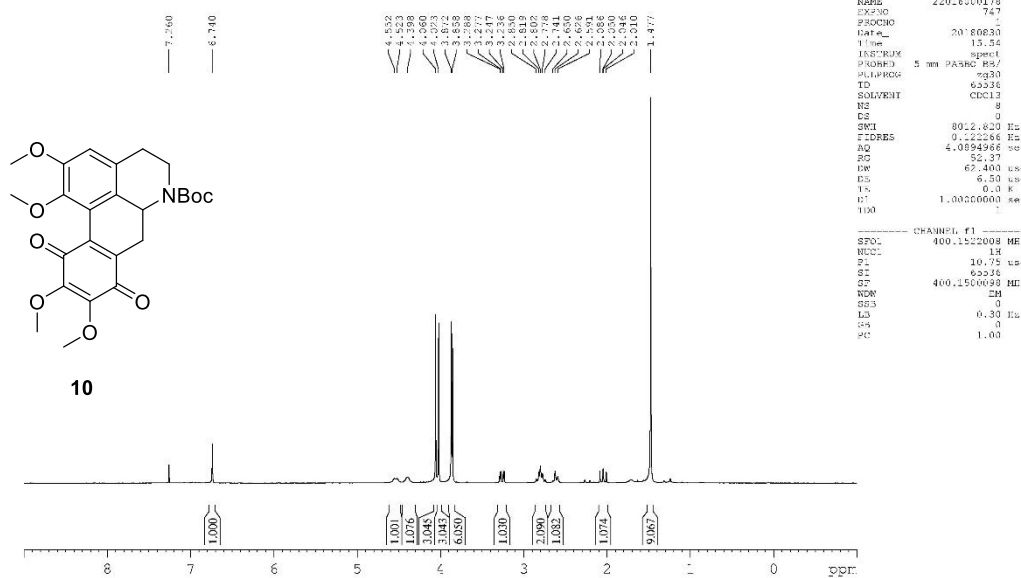
zyj-guanhuan



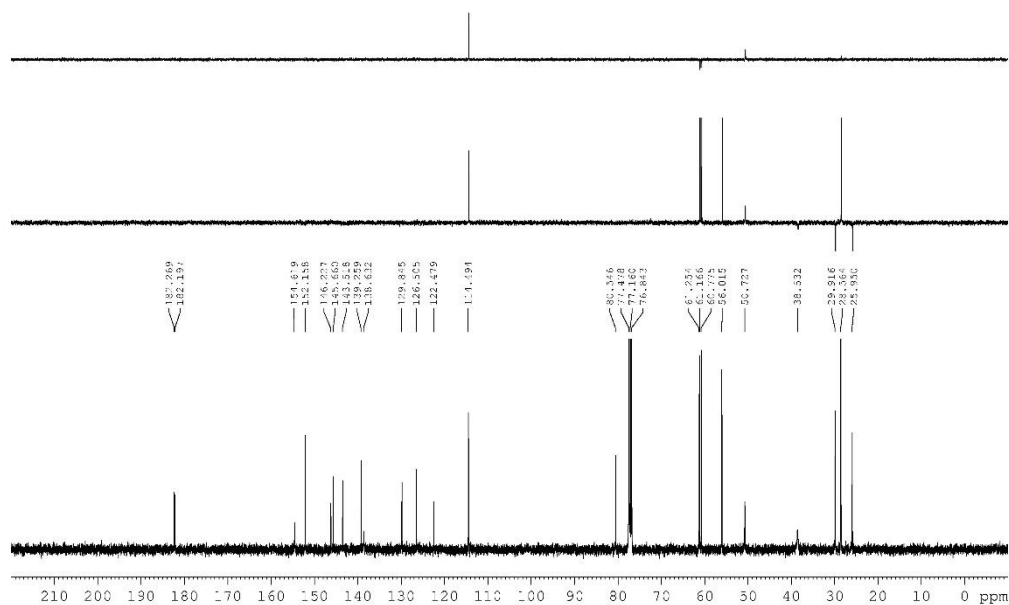
zyj-guanhuan



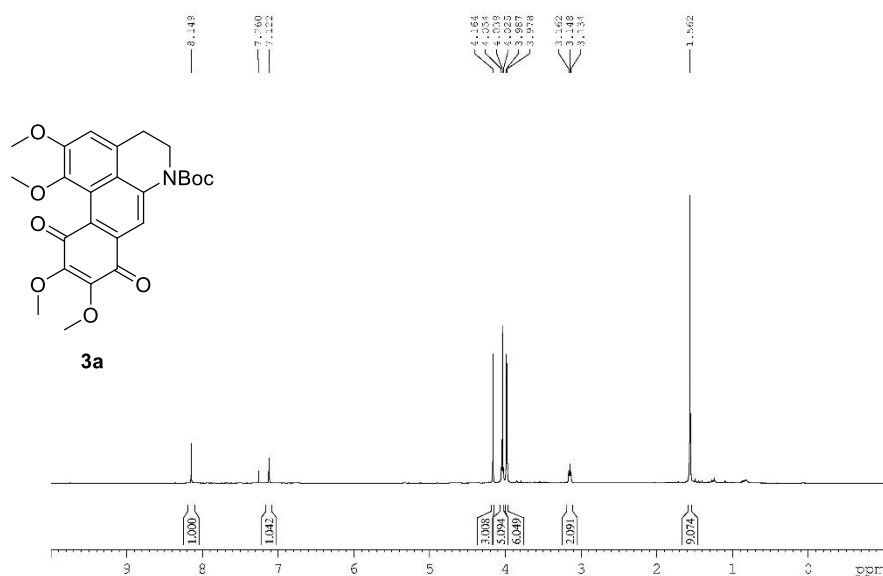
zyj-11-shuangtong



zyj-11-shuangtong



zyj-12-fanggouhua

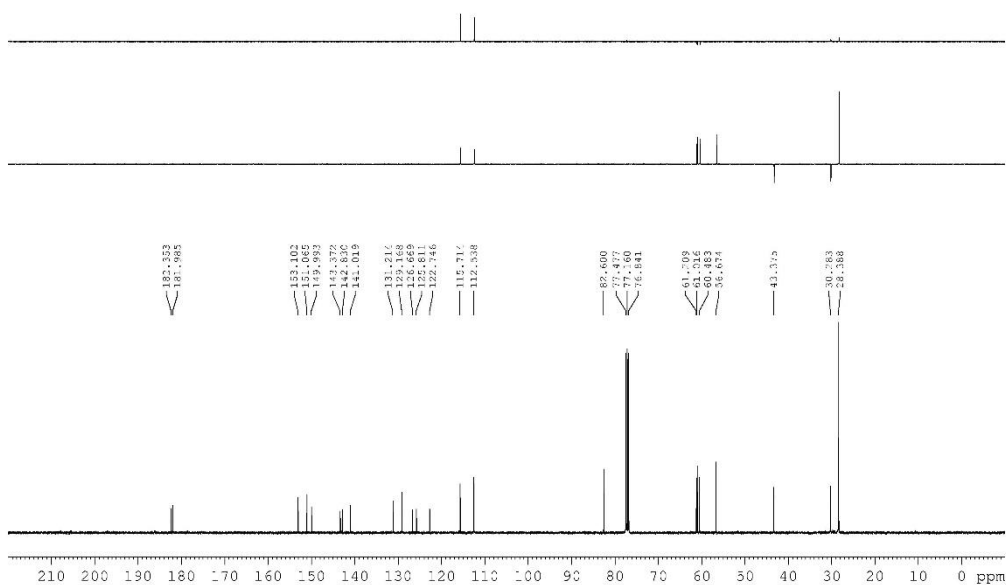


```

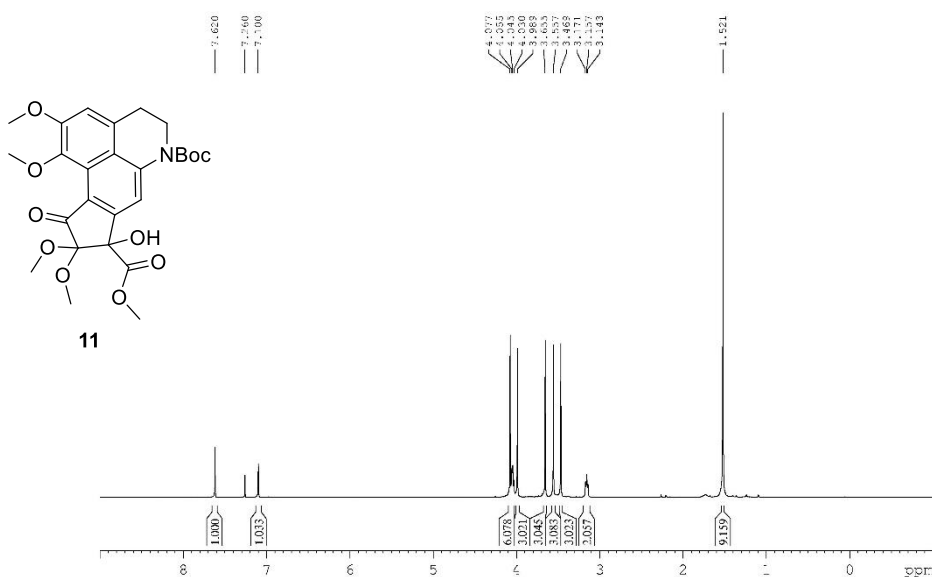
NAME      22016000170
EXPNO     1
PROCNO    1
Date_     20180830
Time      16.27
INSTRUM    spect
PULPROG    zgpg30
TD         65536
SOLVENT    CDCl3
NS          3
DS          4
SWH         8012.620 Hz
FIDRES     0.122266 Hz
AQ         4.0894966 sec
RG          31.56
RW         62.400 Hz
DS         6.50 Hz
TS          0.3 K
RG         1.0020000 sec
NUC1       13
----- CHANNEL f1 -----
SFO1      400.1522008 MHz
NUC1       13
P1         10.75 usec
PL         0.00 dB
SFO2      400.1510005 MHz
NUC2       1H
PC         0.30 usec
PL         0.00 dB
RG         1.00

```

zyj-12-fanggouhua

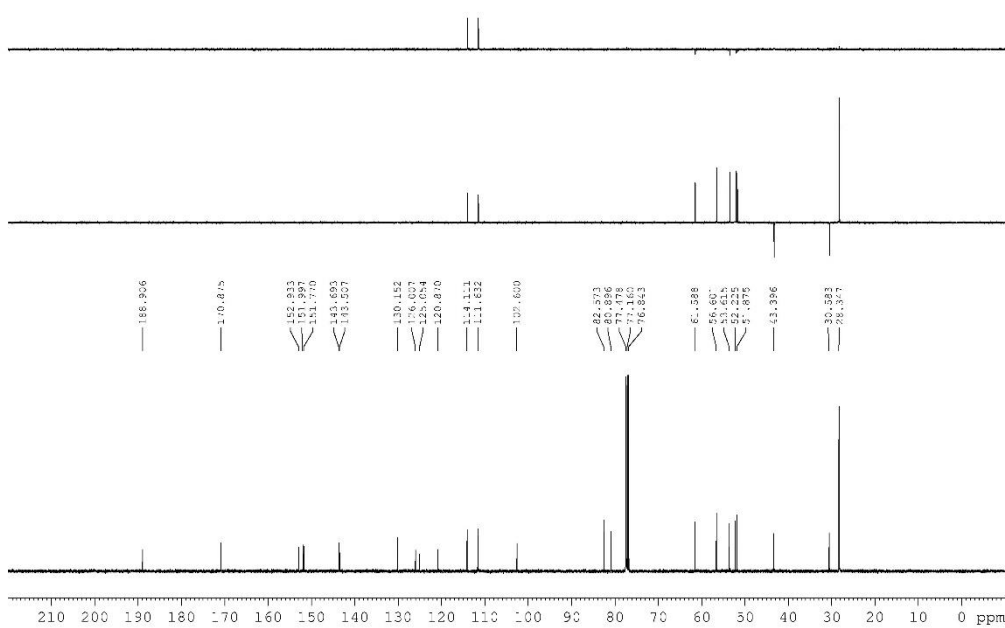


zyj-13-chongpai



NAME 220-6000178
EXPNO 739
PROCNO 1
INSTRUM spect
F1 200.80823
V1 19.53
INSTNUM 5
PULPROG zg30
TD 65536
ID 00013
SOLVENT CDCl₃
NS 8
DS 0
SWH 8012.820 Hz
FIDRES 0.122266 Hz
AQ 4.0894968 sec
RG 53.34
RW 62.400 sec
ES 6.50 sec
TS 0.0 K
D1 1.00200000 sec
T100 0
----- CHANNEL f1 -----
SFO1 400.1512009 MHz
NUC1 13
P1 10.75 sec
PT 4.2356
ST 400.1500095 MHz
RDM 2H
RG 0
L3 0.30 Hz
DS 0
PC 1.00

zyj-13-chongpai



Chemical structure of **11a** is shown above the spectrum. The spectrum displays peaks corresponding to the structure, with integration values and chemical shifts (δ) provided.

Chemical shifts (δ): 7.813, 7.260, 7.175, 4.896, 4.642, 4.622, 4.602, 3.993, 3.973, 3.944, 3.661, 3.641, 3.620, 3.167, 3.148, 3.129, 1.510.

Integration values: 1.00, 1.06, 1.02, 8.71, 3.03, 3.15, 2.05, 9.07.

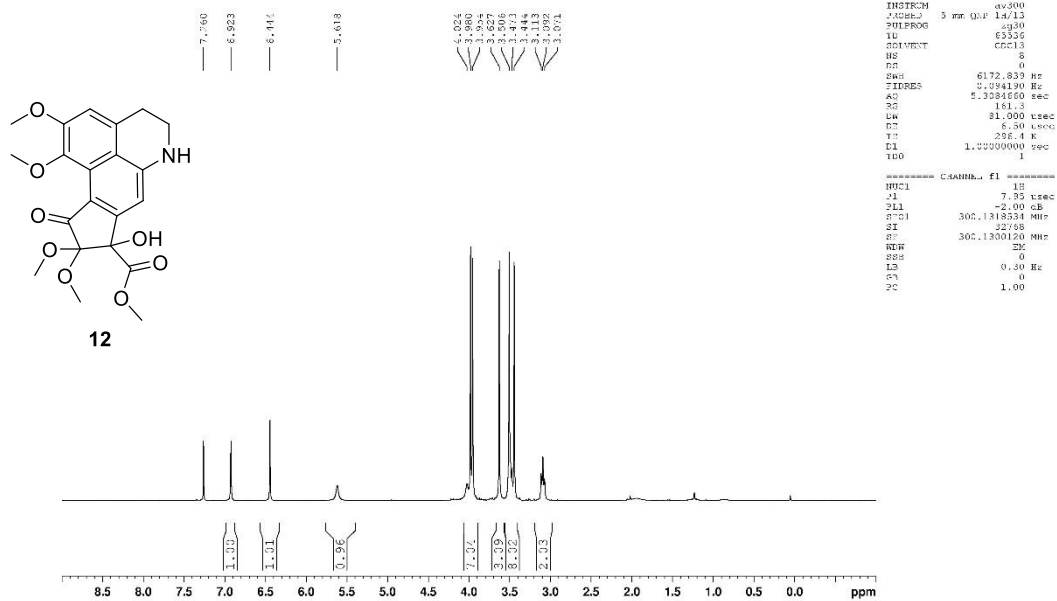
```

>AMN 1201303011Z
>EXP 822
>PROCIO
>DATE 20180326
>TIME 15.19
>LSTENR 1
>FREQ 5 m n GP 107.13
>FREQROF 4937
>F 653.36
>DO-AMN2 03-0033
>C 0
>DC 0
>DMW 6172.830 Hz
>F-DEFS 0.0001 Hz
>RG 4.69466 sec
>WR 181
>RG 28
>DE 81.200 msec
>DE 6.55 msec
>TE 284.6 Hz
>F 1.000321 sec
>=====
>===== CHANNEL #1 =====
>FREQ 1M
>P 7.90
>T -2.20 dB
>SFREQ 300.131875 MHz
>F 337.68
>FREQ 300.1300122 MHz
>WDF
>RNB 1M
>DB 0
>FC 0.03 Hz
>DB 0
>FC 1.00

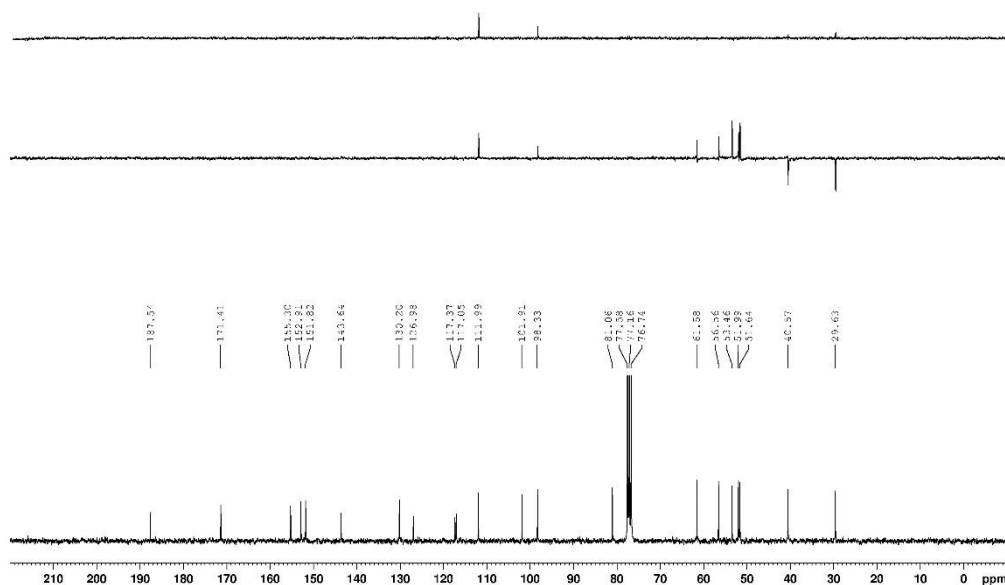
```

¹³C NMR spectrum (CDCl₃) of compound 1. The x-axis represents chemical shift in ppm, ranging from 0 to 210. The spectrum shows several sharp peaks. Key peaks are labeled with their chemical shift values: 194.46, 172.28, 133.16, 129.39, 142.49, 141.94, 138.17, 133.42, 130.32, 124.96, 124.39, 116.76, 116.96, 101.87, 83.78, 82.09, 77.58, 76.71, 61.29, 56.81, 52.27, 52.07, 43.00, 30.63, and 28.38. A cluster of peaks between 70-90 ppm is associated with the solvent CDCl₃.

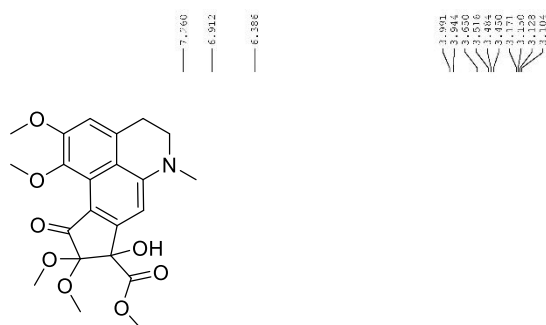
ZYJ-14-TUOBAC



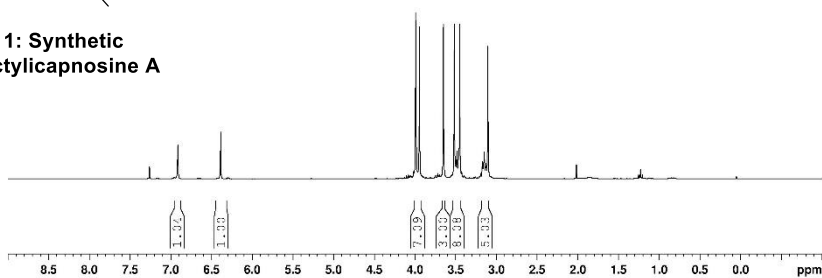
ZYJ-14-TUOBAC



ZUIZHONGCHANWU



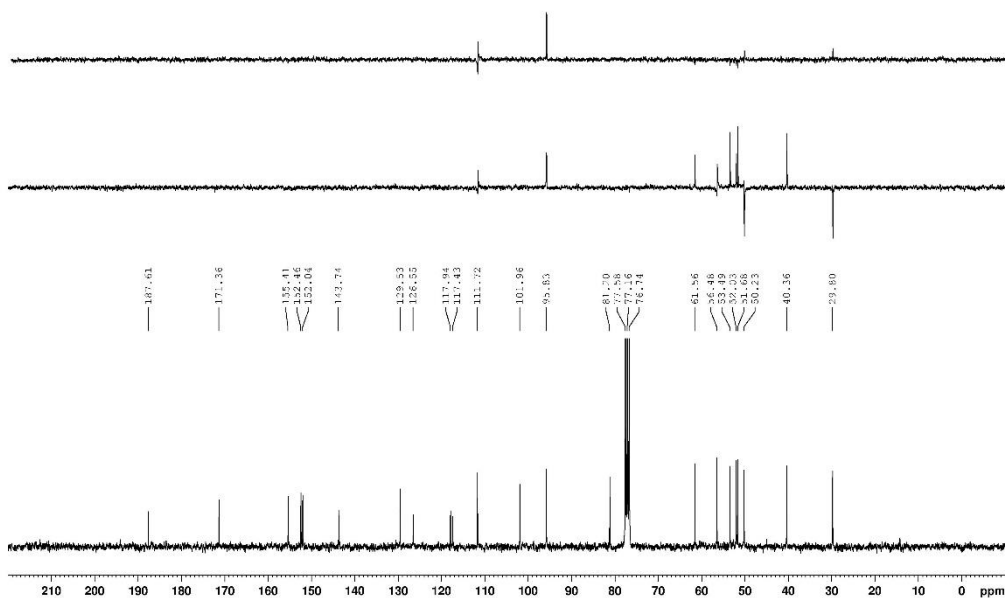
1: Synthetic dactylicapnosine A



```

NAME      12013001120
EXPNO     1001
PROCNO    1
Date_     20180824
Time      20.09
INSTRUM   av300
PROBHD    5 mm QNP
PULPROG   zgpg30
TD         65536
SOLVENT   CDCl3
NS         8
DS         4
SWH        6172.833 Hz
FIDRES     0.094190 Hz
AQ         5.3084600 sec
RG          181
BW         81.000 tsec
DQ         6.30 tsec
TE         295.1 K
D1         1.00000000 sec
DELTA      1
===== CHANNEL f1 =====
NUC1       13
P1         7.95 tsec
PL1        -2.00 dB
NUC2       13
PC1         300.1318334 MHz
SI         32768
SF         300.1300120 MHz
WDW         EM
SSB         0
LB         0.30 Hz
GB         0
PC         1.00
  
```

ZUIZHONGCHANWU



8. Crystal data and structure refinement for dactylicapnosine A (1).

project	data	
Identification code	cu_wd32_0m	
Empirical formula	C ₂₂ H ₂₅ N O ₈	
Formula weight	431.43	
Temperature	100(2) K	
Wavelength	1.54178 Å	
Crystal system	Monoclinic	
Space group	P2 ₁ /c	
Unit cell dimensions	a = 10.5170(10) Å	$\alpha = 90^\circ$.
	b = 12.7338(12) Å	$\beta = 90.699(3)^\circ$.
	c = 14.6646(14) Å	$\gamma = 90^\circ$.
Volume	1963.8(3) Å ³	
Z	4	
Density (calculated)	1.459 Mg/m ³	
Absorption coefficient	0.937 mm ⁻¹	
F(000)	912	
Crystal size	0.380 x 0.350 x 0.170 mm ³	
Theta range for data collection	4.204 to 70.294°.	
Index ranges	-12 ≤ h ≤ 12, -15 ≤ k ≤ 15, -17 ≤ l ≤ 16	
Reflections collected	14698	
Independent reflections	3500 [R(int) = 0.0423]	
Completeness to theta = 67.679°	95.50%	
Absorption correction	Semi-empirical from equivalents	
Refinement method	Full-matrix least-squares on F ²	
Data / restraints / parameters	3500 / 0 / 287	
Goodness-of-fit on F ²	1.069	
Final R indices [I > 2σ(I)]	R1 = 0.0408, wR2 = 0.1061	
R indices (all data)	R1 = 0.0420, wR2 = 0.1078	
Extinction coefficient	n/a	
Largest diff. peak and hole	0.294 and -0.347 e.Å ⁻³	

9. ECD Calculation of dactylicapnosine A (1)

Conformational analysis was initially performed using Confab [5] at MMFF94 force field for the *R*-configuration of compound **1**. Room-temperature equilibrium populations were calculated according to Boltzmann distribution law (eq.1). The energies and populations of all conformers were provided in Table 1. The conformers with Boltzmann-population of over 1% were chosen for ECD calculations.

$$\frac{N_i}{N} = \frac{g_i e^{-\frac{E_i}{k_B T}}}{\sum g_i e^{-\frac{E_i}{k_B T}}} \quad (1)$$

where N_i is the number of conformer i with energy E_i and degeneracy g_i at temperature T , and k_B is Boltzmann constant.

Table S8 Conformational population of R-1 at MMFF94 force field.

Conformer	Energy (kcal/mol)	Population (%)
1	241.1804	100
2	258.4439	0
3	266.6176	0
4	272.2226	0
5	276.3893	0
6	278.1886	0
7	284.1819	0
8	738.8263	0

The theoretical calculation of *R*-configuration **1** were carried out using Gaussian 09 [6]. First, the chosen conformer was optimized at B3LYP/6-311G* using Density functional theory (DFT) (Table). Then, it was further optimized in MeOH using the CPCM polarizable conductor calculation model. The optimized geometry of *R*-**1** was provided in **Table S10**. The theoretical calculation of ECD was conducted using Time-dependent DFT (TD-DFT) method at B3LYP/6-311G* in methanol. Rotatory strengths for a total of 50 excited states were calculated. The ECD spectrum is simulated in SpecDis [7] by overlapping Gaussian functions for each transition according to (eq. 2):

$$\Delta\varepsilon(E) = \frac{1}{2.297 \times 10^{-39}} \times \frac{1}{\sqrt{2\pi}\sigma} \sum_i \Delta E_i R_i e^{-\left(\frac{E-E_i}{2\sigma}\right)^2} \quad (2)$$

where σ represents the width of the band at $1/e$ height, and ΔE_i and R_i are the excitation energies and rotatory strengths for transition i , respectively. $\sigma = 0.25$ eV and UV-Shift = -1 nm and R^{velocity} have been used in this work.

Table S9 Standard orientation of R-1 at B3LYP/6-311G* level in gas phase.

Center Number	Atomic Number	Atomic Type	Coordinates (Angstroms)		
			X	Y	Z
1	6	0	3.418579	-1.366049	0.117328

2	6	0	2.042999	-1.476297	0.093124
3	6	0	1.237069	-0.322732	-0.008246
4	6	0	1.869915	0.943938	-0.138365
5	6	0	3.275511	1.025076	-0.087430
6	6	0	4.027780	-0.107840	0.054028
7	1	0	5.096739	-0.023820	0.086634
8	6	0	1.090171	2.144095	-0.389464
9	7	0	1.749566	3.351620	-0.501939
10	6	0	3.013420	3.477298	0.200575
11	1	0	3.441966	4.440276	-0.042795
12	1	0	2.870311	3.444092	1.281668
13	6	0	3.945623	2.367291	-0.240582
14	1	0	4.209965	2.525132	-1.283082
15	1	0	4.863812	2.397872	0.336732
16	8	0	4.113214	-2.517056	0.190799
17	8	0	1.469276	-2.699354	0.053792
18	6	0	1.491149	-3.469888	1.238424
19	1	0	0.809764	-4.290071	1.079382
20	1	0	1.143298	-2.888050	2.080824
21	1	0	2.487122	-3.845044	1.427525
22	6	0	5.508698	-2.509072	0.088877
23	1	0	5.836290	-2.060431	-0.842675
24	1	0	5.814778	-3.544065	0.110406
25	1	0	5.967756	-1.987287	0.921972
26	6	0	0.964416	4.561063	-0.622611
27	1	0	1.635465	5.398491	-0.753735
28	1	0	0.342177	4.749485	0.251371
29	1	0	0.326614	4.512970	-1.494954
30	6	0	-0.202592	-0.356534	-0.082051
31	6	0	-0.875495	0.789749	-0.381380
32	6	0	-0.265658	2.040290	-0.549363
33	1	0	-0.882400	2.886128	-0.770948
34	6	0	-1.206131	-1.410416	0.193187
35	6	0	-2.504831	-0.946586	-0.507543
36	6	0	-2.382115	0.604457	-0.470983
37	8	0	-1.146734	-2.401925	0.842512
38	8	0	-2.460930	-1.281764	-1.857173
39	8	0	-3.596994	-1.474608	0.127640
40	6	0	-3.085486	1.150895	0.776993
41	8	0	-2.935029	1.240577	-1.568512
42	1	0	-2.755774	0.701756	-2.330409
43	8	0	-4.047579	1.840778	0.760431
44	8	0	-2.485265	0.740584	1.877056
45	6	0	-3.095151	1.074846	3.110984

46	1	0	-4.093550	0.665419	3.157801
47	1	0	-3.139064	2.147571	3.230957
48	1	0	-2.473143	0.634408	3.873539
49	6	0	-2.231102	-2.639983	-2.175667
50	1	0	-2.833366	-3.290070	-1.556423
51	1	0	-1.186013	-2.892601	-2.048955
52	1	0	-2.508696	-2.759613	-3.212872
53	6	0	-4.857902	-1.279562	-0.478366
54	1	0	-4.942327	-1.850763	-1.393928
55	1	0	-5.045434	-0.235967	-0.689119
56	1	0	-5.586138	-1.639247	0.233473

Table S10 Standard orientation of *R*-1 at B3LYP/6-311G* level in solvent phase.

Center Number	Atomic Number	Atomic Type	Coordinates (Angstroms)		
			X	Y	Z
1	6	0	3.459708	-1.339564	0.119903
2	6	0	2.065508	-1.470828	0.081172
3	6	0	1.239205	-0.324623	-0.013760
4	6	0	1.868680	0.963901	-0.147621
5	6	0	3.277361	1.062049	-0.103194
6	6	0	4.052424	-0.070980	0.049239
7	1	0	5.129393	0.028868	0.072863
8	6	0	1.074717	2.155705	-0.402464
9	7	0	1.691897	3.376491	-0.470137
10	6	0	3.011374	3.526458	0.147677
11	1	0	3.415035	4.495366	-0.146169
12	1	0	2.921274	3.519437	1.244115
13	6	0	3.929042	2.406116	-0.311306
14	1	0	4.152683	2.540913	-1.376832
15	1	0	4.878640	2.459331	0.226453
16	8	0	4.168772	-2.497895	0.185067
17	8	0	1.507474	-2.717059	0.010065
18	6	0	1.597416	-3.539384	1.187532
19	1	0	1.033507	-4.443197	0.964040
20	1	0	1.133450	-3.035409	2.036795
21	1	0	2.635934	-3.791540	1.404840
22	6	0	5.595367	-2.436724	0.191535
23	1	0	5.977980	-1.974222	-0.723042
24	1	0	5.931547	-3.470361	0.240801
25	1	0	5.967868	-1.892103	1.064184
26	6	0	0.895385	4.586502	-0.629241
27	1	0	1.569393	5.433110	-0.749388

28	1	0	0.245230	4.775218	0.235249
29	1	0	0.272507	4.523125	-1.523215
30	6	0	-0.200502	-0.378492	-0.091685
31	6	0	-0.896394	0.781080	-0.416390
32	6	0	-0.302062	2.024928	-0.593455
33	1	0	-0.925155	2.877159	-0.819714
34	6	0	-1.178444	-1.428433	0.212338
35	6	0	-2.511650	-0.989067	-0.474748
36	6	0	-2.405069	0.577732	-0.481842
37	8	0	-1.098847	-2.438164	0.880690
38	8	0	-2.502749	-1.337406	-1.848810
39	8	0	-3.591481	-1.541010	0.206401
40	6	0	-3.109855	1.157029	0.760857
41	8	0	-2.995641	1.180048	-1.608780
42	1	0	-2.838738	0.563323	-2.339056
43	8	0	-4.110385	1.826933	0.729421
44	8	0	-2.467533	0.808927	1.880685
45	6	0	-3.074778	1.226067	3.122073
46	1	0	-4.070045	0.791265	3.217452
47	1	0	-3.143840	2.313242	3.161852
48	1	0	-2.418160	0.853633	3.903659
49	6	0	-2.277619	-2.723079	-2.149862
50	1	0	-2.916469	-3.362764	-1.537481
51	1	0	-1.230593	-2.992760	-1.989171
52	1	0	-2.529838	-2.846794	-3.201813
53	6	0	-4.884941	-1.332826	-0.388349
54	1	0	-4.964998	-1.848553	-1.347602
55	1	0	-5.094791	-0.270923	-0.529607
56	1	0	-5.601217	-1.757180	0.313382

References

- (1) Sandor, Z.; Varga, A.; Horvath, P.; Nagy, B.; Szolcsanyi, J., Construction of a stable cell line uniformly expressing the rat TRPV1 receptor. *Cellular & Molecular Biology Letters* **2005**, *10* (3), 499-514.
- (2) Yang, S. L.; Yang, F.; Wei, N. N.; Hong, J.; Li, B. W.; Luo, L.; Rong, M. Q.; Yarov Yarovoy, V.; Zheng, J.; Wang, K. W.; Lai, R., A pain-inducing centipede toxin targets the heat activation machinery of nociceptor TRPV1. *Nature Communications* **2015**, *6*, 8297.
- (3) Abdul Hakim, M.; Jiang, W.; Luo, L.; Li, B.; Yang, S.; Song, Y.; Lai, R., Scorpion toxin, Bmp01, induces pain by targeting TRPV1 channel. *Toxins* **2015**, *7* (9), 3671-3687.
- (4) Numazaki, M.; Tominaga, T.; Takeuchi, K.; Murayama, N.; Toyooka, H.; Tominaga, M., Structural determinant of TRPV1 desensitization interacts with calmodulin. *Proceedings of the National Academy of Sciences of the United States of America* **2003**, *100* (13), 8002-8006.
- (5) Noel M OBoyle, Tim V, ermeersch, Christopher J Flynn, Anita R Maguire Maguire, and Geoffrey

R Hutchison. Confab - systematic generation of diverse low-energy conformers. *Journal of Cheminformatics*, 3:3–8, March **2011**.

(6) M. J. Frisch, G. W. Trucks, H. B. Schlegel, G. E. Scuseria, M. A. Robb, J. R. Cheeseman, G. Scalmani, V. Barone, B. Mennucci, G. A. Petersson, H. Nakatsuji, M. Caricato, X. Li, H. P. Hratchian, A. F. Izmaylov, J. Bloino, G. Zheng, J. L. Sonnenberg, M. Hada, M. Ehara, K. Toyota, R. Fukuda, J. Hasegawa, M. Ishida, T. Nakajima, Y. Honda, O. Kitao, H. Nakai, T. Vreven, J. A. Montgomery, Jr., J. E. Peralta, F. Ogliaro, M. Bearpark, J. J. Heyd, E. Brothers, K. N. Kudin, V. N. Staroverov, R. Kobayashi, J. Normand, K. Raghavachari, A. Rendell, J. C. Burant, S. S. Iyengar, J. Tomasi, M. Cossi, N. Rega, J. M. Millam, M. Klene, J. E. Knox, J. B. Cross, V. Bakken, C. Adamo, J. Jaramillo, R. Gomperts, R. E. Stratmann, O. Yazyev, A. J. Austin, R. Cammi, C. Pomelli, J. W. Ochterski, R. L. Martin, K. Morokuma, V. G. Zakrzewski, G. A. Voth, P. Salvador, J. J. Dannenberg, S. Dapprich, A. D. Daniels, O. Farkas, J. B. Foresman, J. V. Ortiz, J. Cioslowski, and D. J. Fox. Gaussian 09 Revision D.01. Gaussian Inc. Wallingford CT **2009**.

(7) Torsten Bruhn, Anu Schaumlffl, Anu Schaumlffl, Yasmin Hemberger, Yasmin Hemberger, Gerhard Bringmann, and Gerhard Bringmann. Specdis: quantifying the comparison of calculated and experimental electronic circular dichroism spectra. *Chirality*, 25(4):243–249, April **2013**.